


## Research Article

# The Holocene lake-evaporation history of the afro-alpine Lake Garba Guracha in the Bale Mountains, Ethiopia, based on $\delta^{18}\text{O}$ records of sugar biomarker and diatoms

Lucas Bittner<sup>a,b,\*</sup> , Graciela Gil-Romera<sup>c,d</sup>, Dai Grady<sup>e</sup>, Henry F. Lamb<sup>e,f</sup>, Eva Lorenz<sup>a</sup>, Mikaela Weiner<sup>g</sup>, Hanno Meyer<sup>g</sup>, Tobias Bromm<sup>b</sup>, Bruno Glaser<sup>b</sup> and Michael Zech<sup>a</sup>

<sup>a</sup>Heisenberg Chair of Physical Geography with focus on paleoenvironmental research, Institute of Geography, Technische Universität Dresden, 01069 Dresden, Germany; <sup>b</sup>Institute of Agronomy and Nutritional Sciences, Soil Biogeochemistry, Martin-Luther-University Halle-Wittenberg, 06108 Halle (Saale), Germany; <sup>c</sup>Department of Ecology, Philipps-Marburg University, 35037 Marburg, Germany; <sup>d</sup>Department of Geo-environmental Processes and Global Change, Pyrenean Institute of Ecology, CSIC, 50059 Zaragoza, Spain; <sup>e</sup>Department of Geography and Earth Sciences, Aberystwyth University, Aberystwyth SY23 3DB, UK; <sup>f</sup>Department of Botany, School of Natural Sciences, Trinity College Dublin, Dublin 2, Ireland and <sup>g</sup>Alfred Wegener Institute Helmholtz Centre for Polar and Marine Research, Polar Terrestrial Environmental Systems, TelegrafenbergA45, 14473 Potsdam, Germany

### Abstract

In eastern Africa, there are few long, high-quality records of environmental change at high altitudes, inhibiting a broader understanding of regional climate change. We investigated a Holocene lacustrine sediment archive from Lake Garba Guracha, Bale Mountains, Ethiopia, (3,950 m asl), and reconstructed high-altitude lake evaporation history using  $\delta^{18}\text{O}$  records derived from the analysis of compound-specific sugar biomarkers and diatoms. The  $\delta^{18}\text{O}_{\text{diatom}}$  and  $\delta^{18}\text{O}_{\text{fuc}}$  records are clearly correlated and reveal similar ranges (7.9‰ and 7.1‰, respectively). The lowest  $\delta^{18}\text{O}$  values occurred between 10–7 cal ka BP and were followed by a continuous shift towards more positive  $\delta^{18}\text{O}$  values. Due to the aquatic origin of the sugar biomarker and similar trends of  $\delta^{18}\text{O}_{\text{diatom}}$ , we suggest that our lacustrine  $\delta^{18}\text{O}_{\text{fuc}}$  record reflects  $\delta^{18}\text{O}_{\text{lake water}}$ . Therefore, without completely excluding the influence of the ‘amount-effect’ and the ‘source-effect’, we interpret our record to reflect primarily the precipitation-to-evaporation ratio (P/E). We conclude that precipitation increased at the beginning of the Holocene, leading to an overflowing lake between ca. 10 and ca. 8 cal ka BP, indicated by low  $\delta^{18}\text{O}_{\text{lake water}}$  values, which are interpreted as reduced evaporative enrichment. This is followed by a continuous trend towards drier conditions, indicating at least a seasonally closed lake system.

**Keywords:** Paleolimnology, Lake level, Evaporation, Oxygen isotopes,  $\delta^{18}\text{O}$ , Sugar biomarkers, Diatoms

(Received 8 October 2020; accepted 19 March 2021)

### INTRODUCTION

The climate of eastern Africa is driven by the position of the tropical rain belt. Increasing north hemisphere insolation during northern hemisphere summer forces the tropical rain belt and ITCZ northward and the Congo Air Boundary (CAB) migrates eastward (Nakamura, 1968; Hills, 1979; Davies et al., 1985). The eastward extent of CAB movement is related to the seasonal changes of Indian Summer Monsoon (ISM) strength (Camberlin, 1997). Moreover, an increased W-E atmospheric pressure gradient between Africa and India during the northern hemisphere summer enhances the ISM (Wagner et al., 2018). The enhanced ISM redirects Indian Ocean air masses towards India preventing them from penetrating deeply into eastern Africa. Therefore, the convergence zone of Indian Ocean air

masses and Congo Basin air masses shifts to the east (Costa et al., 2014).

In the past, in addition to the effects described above, an increased land-ocean temperature gradient caused strengthening of the West African Monsoon (WAM) and ISM. The interaction of monsoon intensity and eastward migration of the CAB may have been responsible for enhanced moisture in the region, thereby generating a water level rise in eastern African lakes (Junginger et al., 2014; Lezine et al., 2014). Additionally, increased lake levels may have been driven by a northward shift in the mean position of the tropical rain belt during the early Holocene northern hemisphere summer insolation maximum (Gasse, 2000). These processes led to a more pluvial early-mid Holocene (12–5 cal ka BP), termed the African Humid Period (AHP) (deMenocal et al., 2000), which was particularly intense in North Africa and extended south to 10°S in eastern Africa (Gasse, 2000). While the general mechanisms for the orbitally forced AHP are well understood, the spatial and temporal patterns are intensively debated.

Due to the complexity of atmospheric circulation in eastern Africa, it is not surprising that the reconstructed timing of the

\*Corresponding author email address: lucas.bittner@tu-dresden.de

Cite this article: Bittner L et al (2022). The Holocene lake-evaporation history of the afro-alpine Lake Garba Guracha in the Bale Mountains, Ethiopia, based on  $\delta^{18}\text{O}$  records of sugar biomarker and diatoms. *Quaternary Research* 105, 23–36. <https://doi.org/10.1017/qua.2021.26>

AHP differs across sites. The termination of the AHP has been described as rapid (Collins et al., 2017), as synchronous and abrupt (Tierney and deMenocal, 2013), or asynchronous and gradual (Foerster et al., 2012; Costa et al., 2014; van der Lubbe et al., 2017). However, the inferred timing of the AHP termination may depend largely on the analyzed proxy (Castañeda et al., 2016) and the type of archive. Furthermore, in addition to a variable climate, the scarce and patchy paleoenvironmental records of Northern and eastern Africa supply insufficient data for comprehensive climate reconstruction. The hydrological history of eastern Africa has been reconstructed mainly from low-elevation sites.

High-altitude lakes have proved to be excellent sensors of environmental change (Catalan et al., 2006, 2013). They incorporate information about changes in the catchment, including varying erosion, often without significant anthropogenic disturbance or desiccation (Arnaud et al., 2016). In eastern Africa, high-altitude paleolimnological research has been carried out at Lake Ashenge (2442 m asl; Marshall et al., 2009), Lake Dendi (2840 m asl; Wagner et al., 2018), Sacred Lake (2350 m asl on Mount Kenya; Barker et al., 2001, 2011; Street-Perrott et al., 2008; Loomis et al., 2015, 2017), and Lake Garba Guracha (3950 m asl on the Bale Mountains; Umer et al., 2007; Tiercelin et al., 2008; Bittner et al., 2020).

Paleolimnological research has advanced in recent decades by the use of stable isotope ratios as environmental indicators. The oxygen isotope composition ( $\delta^{18}\text{O}$ ) of biogenic compounds and autochthonous carbonates has been established as a valuable paleoclimate proxy because the value of  $\delta^{18}\text{O}$  in water, which is incorporated into biogenic and autochthonous compounds, depends on fractionation processes linked to temperature, air mass source and trajectory, and global ice volume.

Oxygen isotope composition has been determined for several Quaternary records in eastern Africa: for example,  $\delta^{18}\text{O}_{\text{ice}}$  cores (Thompson et al., 2002),  $\delta^{18}\text{O}_{\text{carbonate}}$  (Lamb et al., 2005),  $\delta^{18}\text{O}_{\text{diatom}}$  (Barker et al., 2001, 2007, 2011; Lamb et al., 2005), and  $\delta^{18}\text{O}_{\text{sugar}}$  (Hepp et al., 2017).  $\delta^{18}\text{O}_{\text{sugar}}$  has been successfully applied to several other paleolimnological archives (Zech et al., 2014b; Hepp et al., 2015, 2019). In contrast to this relatively new proxy (Zech and Glaser, 2009), numerous  $\delta^{18}\text{O}_{\text{diatom}}$  records have been published, proving the potential for reconstructing past climate changes from biogenic silica ( $\delta^{18}\text{O}_{\text{diatom}}$ ) (Leng et al., 2001; Barker et al., 2004, 2007, 2011; Lamb et al., 2005; Wilson et al., 2014; Narancic et al., 2016; Cartier et al., 2019; Kostrova et al., 2019).

At Garba Guracha, early work by Umer et al. (2007) and Tiercelin et al. (2008) focused on sedimentological, geochemical, and pollen analyses. Their work indicates that Garba Guracha is one of the longest, most continuous high-resolution Late Quaternary environmental archives from highland Africa. With a new core, Bittner et al. (2020) established a higher resolution chronology and analyzed XRF and biomarkers. Gil-Romera et al. (2019) carried out charcoal and pollen analyses on the same core to show that fire has been a constant disturbance at millennial time scales in the Afromontane vegetation of the Bale Mountains, driving the long-term ecological dynamics of *Erica* spp.

Here we present the first record in eastern Africa of lake-level variation derived from the oxygen isotope composition of sugar biomarkers and diatoms and the first high-altitude, long-term oxygen isotope record from above 3500 m asl in Ethiopia. We compare the results of well-established  $\delta^{18}\text{O}_{\text{diatom}}$  analyses with the more novel  $\delta^{18}\text{O}_{\text{fuc}}$  analyses (Zech and Glaser, 2009) to gain more detailed knowledge regarding the  $\delta^{18}\text{O}_{\text{fuc}}$  proxy and

interpretations of the proxy from the archive itself. Our main aims are: (1) to determine the allochthonous versus autochthonous source of the analyzed sugar biomarkers, (2) to use  $\delta^{18}\text{O}_{\text{diatom}}$  analyses to test and corroborate the  $\delta^{18}\text{O}_{\text{fuc}}$  results, (3) to describe the hydrological history of high-altitude Garba Guracha, and (4) to consider the implications of our data for understanding regional paleoclimate.

## REGIONAL SETTING

### Study area

Garba Guracha is situated in the Bale Mountains of the Bale-Arsi Massif, located east of the Main Ethiopian Rift (Fig. 1). The Sanetti Plateau is the highest plateau in the Bale Mountains at an altitude between ~3800 and ~4200 m asl, encompassing an area of 600 km<sup>2</sup>, bordered by a steep escarpment to the south (Osmaston et al., 2005). Deep valleys incised by northward descending rivers characterize the northern slopes. The volcanic plateau is formed of solidified horizontal lava consisting of alkali basalt, trachyte, and tuffs with rhyolites, overlying older volcanic material (Uhlig and Uhlig, 1991; Williams, 2016). During the Last Glacial Maximum, the plateau and the valleys were locally glaciated (Osmaston et al., 2005; Osendorf et al., 2019; Groos et al., 2020, 2021). The glacial cirque Garba Guracha (6.875781°N, 39.878075°E) (Fig. 2b) was first mentioned by Werdecker (1962) and was described in detail by Umer et al. (2007) and Tiercelin et al. (2008). It is located at 3950 m asl, has a maximum water depth of 6 m, a very small watershed (0.15 km<sup>2</sup>), and extends to ~500 x 300 m in area (Fig. 2c). The catchment bedrock is carbonate-poor (Löffler, 1978; Uhlig and Uhlig, 1991). The lake has an outlet during the rainy season. A marshy alluvial plain fed by several springs extends to the south of the lake.

### Climate

The climate of the Bale Mountains differs from north to south due to differences in altitude, aspect, and continental air masses (Uhlig and Uhlig, 1991; Kidane et al., 2012). The mean annual temperature at Dinsho (Fig. 2a A) is 11.8°C, and the mean minimum temperature for the coldest month is 0.6°C (Hillman, 1986). Ten newly installed climate stations across the Bale Mountains have provided climate data since 2017. The results from 2017 show a mean annual temperature of 4.9°C at the Angesso Station (Fig. 2a B), which is located 4 km northeast of Garba Guracha.

Precipitation in the Bale Mountains originates from two moisture sources, the Indian Ocean monsoon, and the Equatorial Westerlies (Uhlig, 1988; Mieke and Mieke, 1994). A dry season from November to February and a bimodal wet season from March to October define the climate. Precipitation maxima occur in April/May and September/October, respectively (Woldu et al., 1989; Lemma et al., 2020). The highest monthly rainfalls (July to September) are related to the convergence of southwest air masses. In 2017, Angesso Station (3949 m asl) (Fig. 2a B) recorded 1097 mm while 711 mm were registered at the EWCP Station (elevation 4124 m) (Fig. 2a C) and 468 mm at Tulu Dimtu (4385 m asl) (Fig. 2a D). Garba Guracha (3950 m asl) lies at a similar altitude to the Angesso Station. The afro-alpine regions, including the Sanetti Plateau, are characterized by strong diurnal temperature differences between day and night (-15°C to +26°C) (Hillman, 1988).

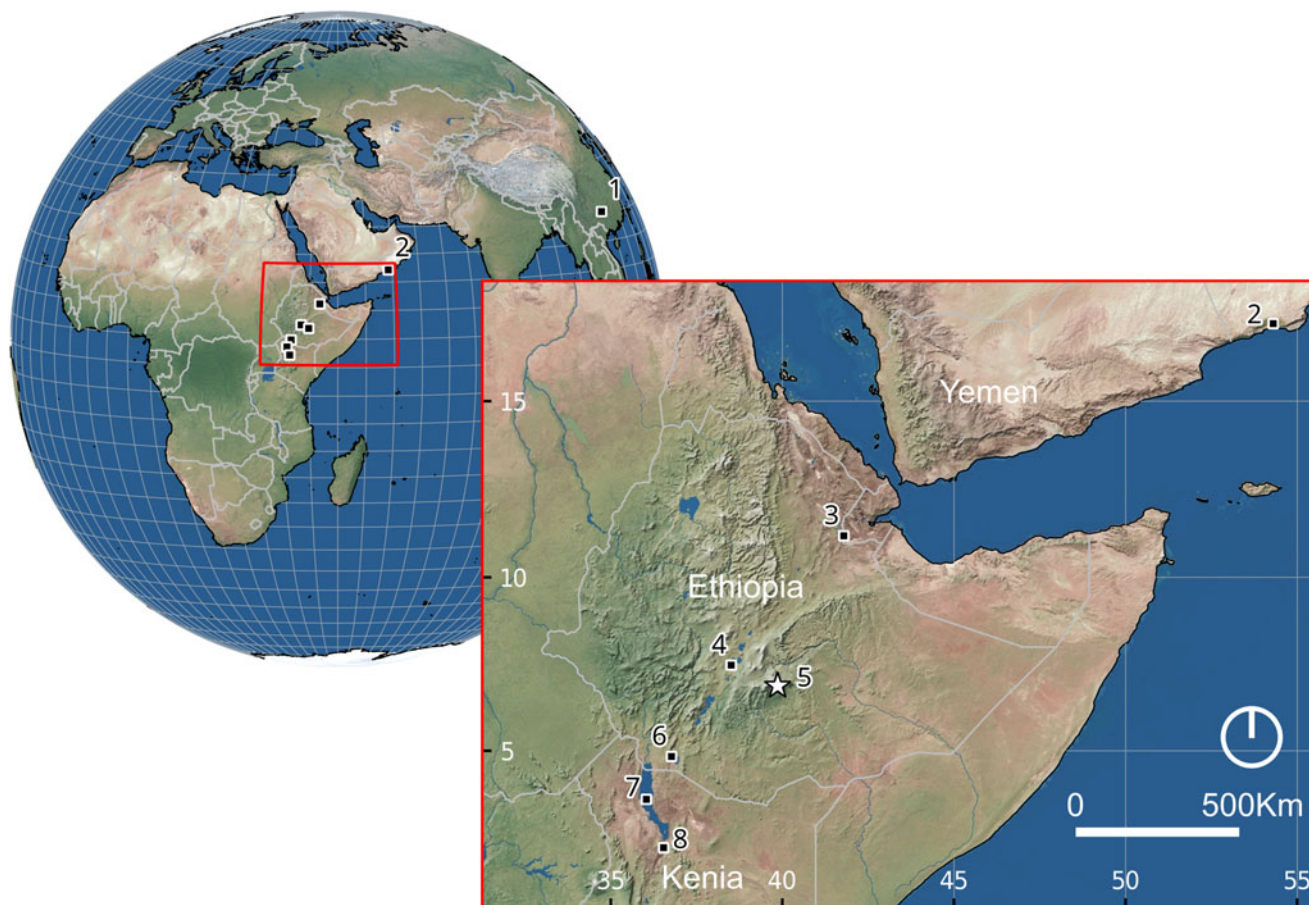


**Figure 1.** Overview of the region: (1) Dongge caves, (2) Qunf cave, (3) Lake Abhè, (4) Ziway-Shala, (5) Garba Guracha (this study), (6) Chew Bahir, (7) Lake Turkana, (8) Paleolake Suguta.

## MATERIAL AND METHODS

### Material and sampling

In February 2017, we retrieved two overlapping sediment cores using a Livingstone piston corer from a raft anchored at 4.8 m water depth. A maximum sediment depth of 1550 cm was reached with an organic-rich upper part (0–900 cm) (Fig. 3) and an organic-poor lower part (900–1550 cm). For radiocarbon dating, we took a total of 31 samples, comprising 18 bulk sediment samples, 8 bulk *n*-alkane, and 5 charcoal samples. More details on sediment and chronology can be found in Bittner et al. (2020). For sugar biomarker analyses ( $n = 80$ ), the organic-rich upper core sections (top 900 cm, compressed to ~800 cm during coring) were sampled at contiguous 10 cm intervals, each sample representing ca. 103 years of sedimentation. This sampling technique enabled us to create a continuous record where variability is smoothed, but without missing information. Nineteen of those samples were later selected for diatom analyses.

### Compound-specific $\delta^{18}\text{O}$ analyses of sugar biomarkers

Sugar biomarker extraction was done at the Institute of Agricultural and Nutritional Sciences, Soil Biogeochemistry, Martin-Luther-University Halle-Wittenberg following the method described by Zech and Glaser (2009). Briefly, monosaccharides were extracted from the homogenized samples by

hydrolysis using 4 M trifluoroacetic acid at 105°C for 4 hours (Amelung et al., 1996). The dissolved monosaccharides were first filtered over glass fiber filters, evaporated, and then further cleaned by transferring them with  $\text{H}_2\text{O}$  onto XAD-7 columns and finally over DOWEX 50WX8 columns. After freeze-drying, the samples were derivatized with methylboronic acid (MBA) for 1 hour at 60°C (Knapp, 1979). The derivatized samples were measured in triplicates on a Trace GC 2000 coupled to a Delta V Advantage IRMS via an  $^{18}\text{O}$ -pyrolysis reactor (GC IsoLink) and a ConFlow IV interface (all devices from Thermo Fisher Scientific, Bremen, Germany). Sugar standards with known  $\delta^{18}\text{O}$  values, containing arabinose (ara), fucose (fuc), and xylose (xyl), were measured in various concentrations after every six sample triplicates (Zech and Glaser, 2009). Correction of the sample  $\delta^{18}\text{O}$  values was applied for possible amount dependency and drift during a sample batch and for the hydrolytically exchangeable oxygen atoms of the carbonyl group (Zech and Glaser, 2009). The  $\delta^{18}\text{O}$  values of the monosaccharides are presented in the usual  $\delta$ -notation versus the Vienna Standard Mean Ocean Water (VSMOW).

### $\delta^{18}\text{O}$ analyses of diatoms

Nineteen sediment samples were processed for diatom oxygen isotope ( $\delta^{18}\text{O}_{\text{diatom}}$ ) analyses. Two g of dry sediment were used to purify samples using a multi-step cleaning procedure.

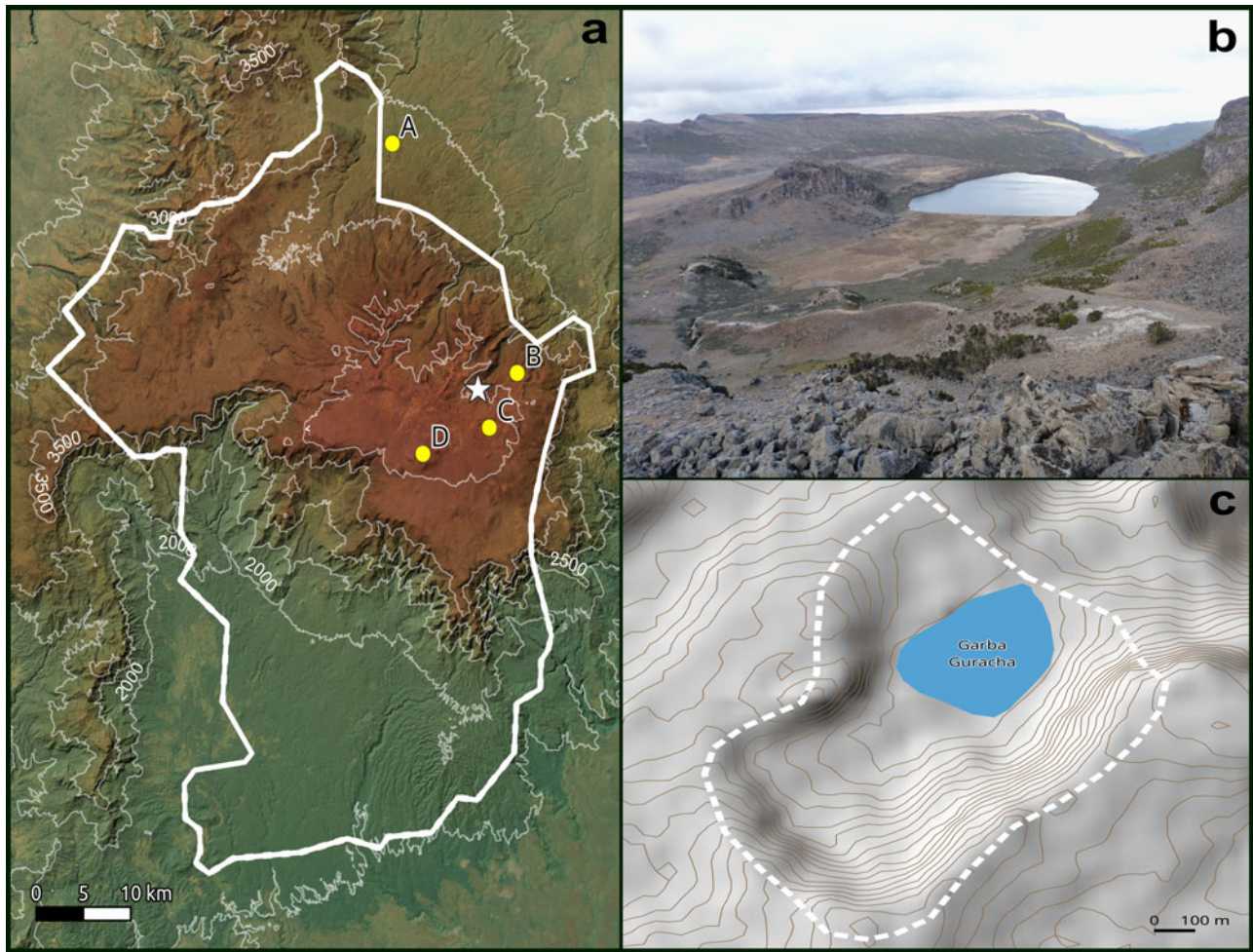


**Figure 2.** Location of the study area. (a) Bale Mountain National Park (thick white line); climate stations: (A) Dinsho, (B) Angesso station, (C) EWCP station, (D) Tulu Dimtu; (b) northeastward view over the glacial cirque of the Garba Guracha catchment; (c) Garba Guracha catchment structure and watershed (dashed white line).

Sediment samples were first treated with 35%  $\text{H}_2\text{O}_2$  on a heating plate at  $50^\circ\text{C}$  for 72 hours to remove organic matter, adding 10% HCl at  $50^\circ\text{C}$  to eliminate carbonates, then washed pH neutral. The subsequent heavy liquid separation was carried out with sodium polytungstate (SPT;  $3\text{Na}_2\text{WO}_4 \cdot 9\text{WO}_3 \cdot \text{H}_2\text{O}$ ) heavy liquid solutions with decreasing densities (2.50–2.05 g/ml) and subsequent centrifuging at 2500 rpm for 30 minutes, leading to the separation of diatoms from heavier detrital contaminants. Decreasing densities were subsequently used to properly separate diatoms from the mineral particles of the terrigenous fraction. Different diatom species have slightly different densities, which makes this step-wise separation procedure necessary in order not to lose any diatoms during heavy liquid separation. This detritus was retained for contamination assessment and used for  $\delta^{18}\text{O}_{\text{diatom}}$  correction following Chaplignin et al. (2010). Diatom samples were washed in ultra-pure water at 2500 rpm for 20 minutes and sieved through a  $3\ \mu\text{m}$  filter. Sixteen of the purified diatom samples ( $n = 19$ ) yielded enough material ( $>1.5\ \text{mg}$ ) to be measured for  $\delta^{18}\text{O}$  at the AWI Potsdam ISOLAB Facility.

To remove exchangeable oxygen, inert Gas Flow Dehydration (iGFD) and heating to  $1100^\circ\text{C}$  under Argon gas (following Chaplignin et al., 2010) was applied. Dehydrated samples were then quantitatively reacted to liberate  $\text{O}_2$  by laser fluorination

under  $\text{BrF}_5$  atmosphere (Clayton and Mayeda, 1963). Sample oxygen was directly measured against a calibrated oxygen reference with a PDZ Europa 2020 mass spectrometer. The working standard BFC ( $\delta^{18}\text{O} = 29.0 \pm 0.3\text{‰}$ ; Chaplignin et al., 2011) was used for calibration (this study:  $\delta^{18}\text{O} = +28.88 \pm 0.24\text{‰}$ ;  $n = 10$ ) for controlling both accuracy and precision of the isotope analyses. The long-term analytical reproducibility ( $1\sigma$ ) is  $\pm 0.25\text{‰}$  (Chaplignin et al., 2010). All measured diatom  $\delta^{18}\text{O}$  values were corrected for contamination, mainly due to clay particles (Supplementary Material Fig. 7), using a geochemical mass-balance approach (Chaplignin et al., 2012). Contamination was calculated for all samples individually and corrected following the method described in Chaplignin et al. (2012). Briefly, we calculated the correction following Equation 2 in Chaplignin et al. (2012):

$$\delta^{18}\text{O}_{\text{corr}} = \delta^{18}\text{O}_{\text{measured}} + (\% \text{cont.} \times \delta^{18}\text{O}_{\text{cont.}})$$

where  $\delta^{18}\text{O}_{\text{measured}}$  is the isotopic composition of the sample after purification, %cont. is the contamination percentage left in the purified sample and  $\delta^{18}\text{O}_{\text{cont.}}$  is the isotopic composition of the contaminants (i.e., the heavy [mineral] fraction).

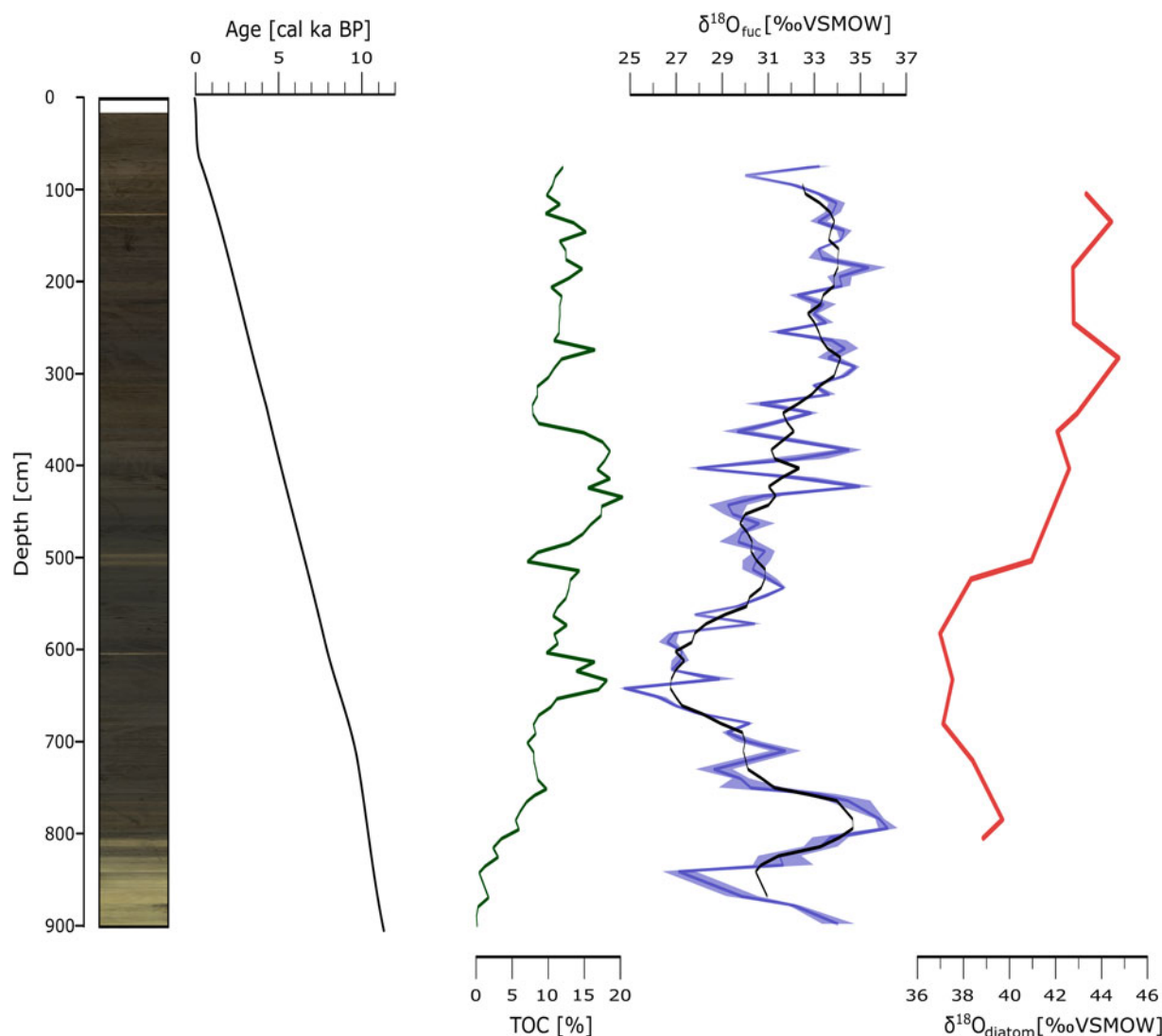


**Figure 3.** Depth profiles of age and TOC (Bittner et al., 2020),  $\delta^{18}\text{O}_{\text{fuc}}$  (blue), and  $\delta^{18}\text{O}_{\text{diatom}}$  (purple) (this study). The black line shows the running mean of 5. Stacked core photos are shown on the left and shaded areas indicate the standard error range.

## RESULTS

### $\delta^{18}\text{O}_{\text{fuc}}$ record of Garba Guracha

Compound-specific  $\delta^{18}\text{O}$  values for the sugar biomarker fucose reveal a total range from +24.7 to +36.2‰ (Fig. 3). The mean standard error for fucose was  $\pm 1.4\text{‰}$ . The  $\delta^{18}\text{O}$  values of fucose increase from 840 cm (11 cal ka BP) and begin to decrease at ~800 cm (10.5 cal ka BP) showing minima between 665 and 535 cm (9 and 7 cal ka BP). Thereafter, a continuous trend towards more positive  $\delta^{18}\text{O}$  values of fucose is apparent until 290 cm (3.5 cal ka BP). Above this depth, stable values continue with the exception of one pronounced minimum at ~85 cm (0.5 cal ka BP).

In detail, the Early Holocene reveals centennial-scale  $\delta^{18}\text{O}_{\text{fuc}}$  shifts with minima at 840 and 750 cm (10.9 and 10.2 cal ka BP), and a maximum at 800 cm (10.6 cal ka BP). The phase of lowest  $\delta^{18}\text{O}_{\text{fuc}}$  values is interrupted by a short maximum at 635 cm (8.4 cal ka BP). The Late Holocene reveals major fluctuations of  $\delta^{18}\text{O}_{\text{fuc}}$  between 425 and 370 cm (5.5 and 4.6 cal ka BP).

Moreover, a maximum at 290 cm (3.5 cal ka BP), a minimum at 85 cm (0.5 cal ka BP), and numerous centennial-scale variations are visible in the Late Holocene. However, the variability of  $\delta^{18}\text{O}$  is highest during the Early Holocene and decreases towards the Late Holocene.

### $\delta^{18}\text{O}_{\text{diatom}}$ record of Garba Guracha

For most of the 16 diatom samples, duplicate or triplicate oxygen isotope analyses yielded a mean (max) standard deviation of  $\pm 0.26\text{‰}$  ( $\pm 0.51\text{‰}$ ; Supplemental Table 1). One sample could only be measured once due to low diatom content after the separation procedure. In general, the  $\delta^{18}\text{O}_{\text{diatom}}$  values span a range of 7.9‰ (Fig. 3). Like the  $\delta^{18}\text{O}_{\text{fuc}}$  data, the  $\delta^{18}\text{O}_{\text{diatom}}$  values decrease above 750 cm (10 cal ka BP), with lowest values co-occurring between 665 and 535 cm (9 and 7 cal ka BP) ( $\delta^{18}\text{O}_{\text{diatom}} \sim +37\text{‰}$ ). An overall increasing trend between 535 and 285 cm (7 and 3.5 cal ka BP) is interrupted by a decrease between 425 and 370 cm (5.5 and 4.6 cal ka BP). More less-

positive values follow the maximum at 285 cm (3.5 cal ka BP) ( $\delta^{18}\text{O}_{\text{diatom}} = +44.8\text{‰}$ ) until 140 cm. A small maximum at 140 cm (1.5 cal ka BP) and subsequent decreasing values are similar to the  $\delta^{18}\text{O}_{\text{fuc}}$  record.

## DISCUSSION

### *The Garba Guracha $\delta^{18}\text{O}_{\text{fuc}}$ record - lake or leaf water?*

A crucial issue for the interpretation of  $\delta^{18}\text{O}_{\text{fuc}}$  records is the aquatic (autochthonous) or terrestrial (allochthonous) origin of the sedimentary sugar biomarkers. Plant-derived sugar biomarkers, modified by a biosynthetic fractionation factor ( $\epsilon_{\text{bio}}$ ), can either reflect lake water  $\delta^{18}\text{O}$  ( $\delta^{18}\text{O}_{\text{lake water}}$ ) or terrestrial leaf water  $\delta^{18}\text{O}$  ( $\delta^{18}\text{O}_{\text{leaf water}}$ ) origin. In the case of Garba Guracha, a high aquatic organic matter content of the sediments can be inferred from several proxies. First, relatively positive  $\delta^{13}\text{C}$  values of  $> -23\text{‰}$  and a low TOC/N ratio of  $<15$  indicate a high aquatic organic matter content (Bittner et al., 2020). Second, the sugar biomarker quantification pattern indicates a high relative abundance of fucose in the Garba Guracha sediments. Fucose is a major component of phytoplankton, zooplankton, and bacteria (Ogier et al., 2001), as well as of aquatic plants (Hepp et al., 2016). In terrestrial vascular plants, fucose is produced in low concentrations, according to Hepp et al. (2016) who developed two ratios, fuc/(ara + xyl) and (fuc + xyl)/ara, to distinguish between aquatic ( $> 0.10$ ) and terrestrial ( $\leq 0.10$ ) input. In our data, both ratios suggest that the sediments of Garba Guracha contain sugar biomarkers that are principally of aquatic origin (Bittner et al., 2020, Fig. 6). While a partial terrestrial contribution of sugar biomarkers to the sediments cannot be fully excluded, the terrestrial contribution, especially of fucose, can be neglected. We therefore interpret our  $\delta^{18}\text{O}_{\text{fuc}}$  data as a record of changes in  $\delta^{18}\text{O}_{\text{lake water}}$ .

### *The Garba Guracha $\delta^{18}\text{O}_{\text{diatom}}$ record*

$\delta^{18}\text{O}_{\text{lake water}}$  and temperature at the time of frustule formation define the  $\delta^{18}\text{O}_{\text{diatom}}$  composition of aquatic diatoms (Labeyrie, 1974; Leclerc and Labeyrie, 1987; Leng and Barker, 2006). Some processes in the incorporation of oxygen isotopes into diatom silica (summarized by Bird et al., 2020) still require a better understanding, such as (1) species-specific fractionation (Bailey et al., 2014), (2) post-mortem alteration of the oxygen isotopic composition (Tyler et al., 2017), and (3) the effect of diagenesis on oxygen isotope fractionation and exchange (Dodd et al., 2012). However,  $\delta^{18}\text{O}_{\text{diatom}}$  analyses have been applied successfully to many archives as a proxy for P/E to identify wet and dry conditions (Polissar et al., 2006; Meyer et al., 2015), moisture source (Rosqvist et al., 2004; Leng et al., 2005; Schiff et al., 2009),  $\delta^{18}\text{O}_{\text{precipitation}}$  (Morley et al., 2005; Mackay et al., 2013; Bailey et al., 2015), hydrological changes (Narancic et al., 2016; Kostrova et al., 2019), and temperature (Kostrova et al., 2014). The interpretation of  $\delta^{18}\text{O}_{\text{diatom}}$  as a proxy for temperature is difficult due to the variability of  $\delta^{18}\text{O}_{\text{precipitation}}$  and, especially in warm and/or dry environments, due to evaporative enrichment. These factors may have a more significant influence on  $\delta^{18}\text{O}_{\text{diatom}}$  than temperature (Leng and Barker, 2006). Especially in the tropics, where inter-annual and seasonal temperature variability is low,  $\delta^{18}\text{O}_{\text{diatom}}$  generally has been interpreted as a proxy for precipitation amount (Cole et al., 1999; Lamb et al., 2005; Barker et al., 2007). Barker et al. (2001) suggested that the

$\delta^{18}\text{O}_{\text{diatom}}$  record of Small Hall Tarn and Simba Tarn at Mount Kenya represents the moisture balance of lake-level stands and overflows.

For reconstructing the  $\delta^{18}\text{O}_{\text{lake water}}$ , several calibration studies for modern diatoms (Brandriss et al., 1998; Moschen et al., 2005; Crespin et al., 2010; Dodd and Sharp, 2010) and one for sedimentary diatoms (Leclerc and Labeyrie, 1987) have been published. The temperature-coefficient of these studies is quite similar ( $-0.16\text{‰}/^{\circ}\text{C}$  to  $-0.29\text{‰}/^{\circ}\text{C}$ ), although offsets of several per mil between the regression lines are present. Explanations suggested by Crespin et al. (2010) include (1) an under- or overestimation of temperature or  $\delta^{18}\text{O}_{\text{lake water}}$  in the calibration, (2) incomplete accounting for exchangeable oxygen, and (3) post-mortem  $^{18}\text{O}$  enrichment of sedimentary diatoms (Schmidt et al., 2001). To account for post-mortem  $^{18}\text{O}$  enrichment, we reconstructed the  $\delta^{18}\text{O}_{\text{lake water}}$  of the Garba Guracha sedimentary diatoms using the equation of Leclerc and Labeyrie (1987). Taking into consideration a mean annual  $T_{\text{air}}$  of  $\sim 4.9^{\circ}\text{C}$  (min:  $3.5^{\circ}\text{C}$ , max:  $6.0^{\circ}\text{C}$ ) in 2017, measured at the closest meteorological station (Angesso), which is at the same altitude as Lake Garba Guracha, an isotope fractionation factor  $\alpha$  in the system (silica-water) of  $1.0435 \pm 0.004$  can be calculated (Leclerc and Labeyrie, 1987). The calculated value is subject to some uncertainty due to the lack of more recent  $\delta^{18}\text{O}_{\text{diatom}}$  values, an incomplete record of modern  $\delta^{18}\text{O}_{\text{lake water}}$  variability, and an underestimation of frustule growth temperature by using mean annual air temperature.

Based on these factors, the measured most recent (931 cal. BP)  $\delta^{18}\text{O}_{\text{diatom}}$  of  $\sim +43.4\text{‰}$  at Lake Garba Guracha leads to a calculated “modern”  $\delta^{18}\text{O}_{\text{lake water}}$  value of  $+0.8 \pm 0.3\text{‰}$ , which is lower than the measured  $\delta^{18}\text{O}_{\text{lake water}}$  of  $+4.7\text{‰}$  at the end of the 2017 dry season, representing strong  $^{18}\text{O}$  enrichment of lake water (Lemma et al., 2020). For comparison, precipitation in 2017 yielded a mean  $\delta^{18}\text{O}$  value of  $-4.5\text{‰}$  (max  $-6.2\text{‰}$ , min  $-1.9\text{‰}$ ). The reconstructed  $\delta^{18}\text{O}_{\text{lake water}}$  value of  $+0.8\text{‰}$  for the uppermost diatom sample is hence a reasonable estimated value between those of modern precipitation ( $-4.5\text{‰}$ ) and the seasonally enriched lake water ( $+4.7\text{‰}$ ) (Lemma et al., 2020).

### *Comparison of reconstructed $\delta^{18}\text{O}_{\text{lake water}}$ from $\delta^{18}\text{O}_{\text{fuc}}$ versus $\delta^{18}\text{O}_{\text{diatom}}$*

The predominantly aquatic origin of sugar biomarkers in the Garba Guracha sediments, as discussed earlier, leads to the conclusion that the isotopic composition of the fucose sugar biomarkers primarily represents  $\delta^{18}\text{O}_{\text{lake water}}$  modified by  $\epsilon_{\text{bio}}$ , the biosynthetic fractionation factor.  $\epsilon_{\text{bio}}$  can be estimated as  $+29\text{‰}$  between aquatic cellulose  $\delta^{18}\text{O}$  and  $\delta^{18}\text{O}_{\text{lake water}}$  (Mayr et al., 2015). An  $\epsilon_{\text{bio}}$  of  $+29\text{‰}$  may slightly underestimate the fractionation factor of aquatic hemicellulose, as is known for terrestrial cellulose and hemicellulose (Zech et al., 2014a, b; Hepp et al., 2019). The slight offset derives from the loss of the relatively  $^{18}\text{O}$ -depleted oxygen atom attached to C-6 during 6-deoxyhexose (fucose) biosynthesis (C-6 decarboxylation; Altermatt and Neish, 1956; Harper and Bar-Peled, 2002; Burget et al., 2003). This is supported by the findings of Waterhouse et al. (2013) that  $\sim 80\%$  of the oxygen atoms at the C-6 position are isotopically exchanged during cellulose synthesis. Similarly, the Garba Guracha  $\delta^{18}\text{O}_{\text{diatom}}$  record can be interpreted as  $\delta^{18}\text{O}_{\text{lake water}}$  due to a lesser influence of temperature in tropical regions, as discussed previously.

The reconstructed  $\delta^{18}\text{O}_{\text{lake water}}$  values of sugar biomarker and diatoms are consistent after correction for  $\epsilon_{\text{bio}}$  ( $+29\text{‰}$ ) (Mayr

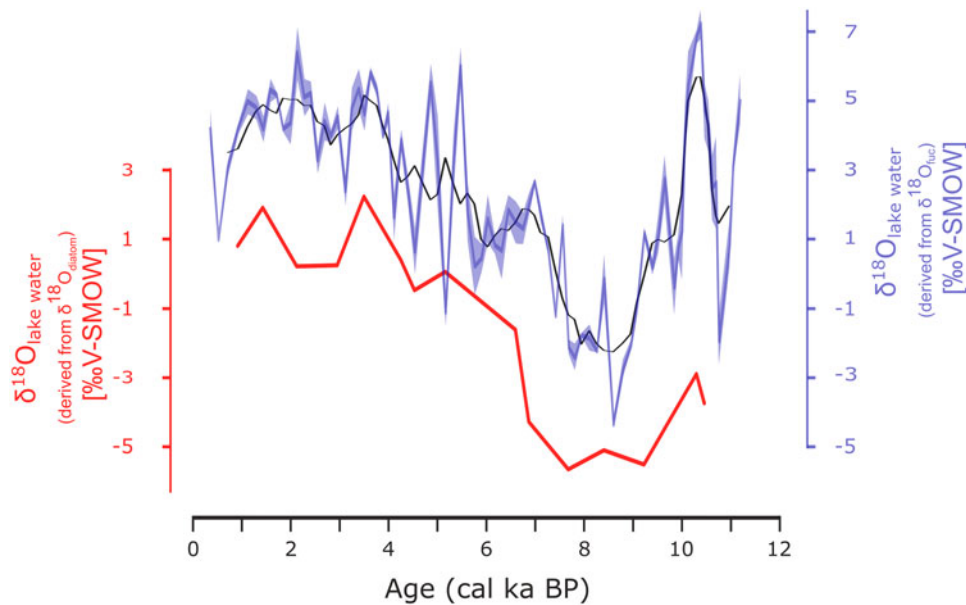


**Figure 4.** Comparison of the  $\delta^{18}\text{O}_{\text{diatom}}$  and  $\delta^{18}\text{O}_{\text{fucose}}$  records of Garba Guracha. The black line shows the running mean of 5 and shaded areas the standard error range.

et al., 2015) and temperature-dependent fractionation during diatom growth (Leclerc and Labeyrie, 1987), respectively (Fig. 4). Additionally, the  $\delta^{18}\text{O}_{\text{diatom}}$  and  $\delta^{18}\text{O}_{\text{fucose}}$  ranges of the 16 analyzed samples are similar (7.9‰ and 7.1‰, respectively). Despite the rather small number of analyses, the aquatic  $\delta^{18}\text{O}_{\text{diatom}}$  and  $\delta^{18}\text{O}_{\text{fucose}}$  show identical trends during the Holocene (Fig. 3), pointing to a common source of  $\delta^{18}\text{O}_{\text{fucose}}$  and  $\delta^{18}\text{O}_{\text{diatom}}$ . Therefore, we conclude that the  $\delta^{18}\text{O}_{\text{diatom}}$  record corroborates the  $\delta^{18}\text{O}_{\text{fucose}}$  record to reflect primarily  $\delta^{18}\text{O}_{\text{lake water}}$  and, moreover, that  $\delta^{18}\text{O}_{\text{fucose}}$  of aquatic sugar biomarker is a valuable proxy for  $\delta^{18}\text{O}_{\text{lake water}}$  in the Garba Guracha sedimentary archive.

#### Paleoclimatic significance and proxy interpretation

Past variations of  $\delta^{18}\text{O}_{\text{lake water}}$  reflect past changes in  $\delta^{18}\text{O}_{\text{precipitation}}$  and evaporative  $^{18}\text{O}$  enrichment of lake water. In the tropics,  $\delta^{18}\text{O}_{\text{precipitation}}$  values in paleo-archives and rainfall records have been interpreted to represent changes in the amount of precipitation—depleted  $\delta^{18}\text{O}$  values indicating high amounts of precipitation (amount effect; Dansgaard, 1964; Rozanski et al., 1993). However, besides amount effect, the history of the entire moist air mass, including source region (source effect), the air mass convection (altitude effect), (re)evaporative history (recycling), and transport distance (continental effect), must be considered (Sharp, 2017). Moreover,  $\delta^{18}\text{O}_{\text{precipitation}}$  is influenced by temperature (temperature effect; Rozanski et al., 1993). However, temperature changes in the tropics, especially during the Holocene, were rather small (Berke et al., 2012), implying that the temperature effect is negligible (Rozanski et al., 1993; Vuille et al., 2005).

The relatively small temperature effect means that  $\delta^{18}\text{O}_{\text{precipitation}}$  is predominantly influenced by the amount and the source effect in eastern Africa. For the tropics in general, high-resolution  $\delta^{18}\text{O}$  speleothem records, such as those of Fleitmann et al. (2003) and Dykoski et al. (2005) (Fig. 5), are generally interpreted as mainly reflecting variations in the intensity of the monsoon systems (amount effect)—East Asian Summer (EASM) and

the Indian Summer Monsoon (ISM). Overall trends of Qunf cave  $\delta^{18}\text{O}$  (Fleitmann et al., 2003) and Dongge cave  $\delta^{18}\text{O}$  (Dykoski et al., 2005) are in agreement with our  $\delta^{18}\text{O}$  records (Fig. 5). Monsoon intensity in eastern Africa may have played an essential role in controlling the stable isotope composition of precipitation, as recorded in our Bale Mountain archive and reconstructed  $\delta^{18}\text{O}$  values. However, modern data suggest that the amount effect alone does not explain the  $\delta^{18}\text{O}_{\text{precipitation}}$  pattern in eastern Africa (Costa et al., 2014; Lemma et al., 2020). Therefore, Costa et al. (2014) questioned the primary influence of the amount effect for Lake Tana, Ethiopia, and suggested that an Atlantic moisture source (Congo Basin) was responsible for both past and current depleted  $\delta^{18}\text{O}_{\text{precipitation}}$  values. Back-trajectories for modern precipitation at Lake Tana show an average contribution from Congo Basin air masses of 13%. The primary source is the Indian Ocean (80%), with only a minor contribution of 7% from the Mediterranean and Red Sea (Costa et al., 2014). Other climate studies for Ethiopia have found only minor (Viste and Sorteberg, 2013) or no (Levin et al., 2009) air mass contributions to southern Ethiopia from the Congo Basin. However, a recent study by Finney et al. (2020) suggests that despite the low air mass contribution, westerly winds are responsible for a disproportionately high amount of rainfall in eastern Africa. For the Bale Mountains, a recent back-trajectory study found air mass contributions principally from the Indian Ocean and the Mediterranean and Red Sea, but no evidence for any contribution or even an isotopic depletion due to Congo Basin air masses (Lemma et al., 2020).

Even if these air mass contributions are not nowadays influencing rainfall in southeastern Ethiopia (Levin et al., 2009) or the Bale Mountains (Lemma et al., 2020), a past change of atmospheric circulation could have exerted a significant effect on the isotopic composition of paleo records (Tierney et al., 2011a; Junginger et al., 2014). We, however, have no further evidence to test potential past source contributions at our study site. A change in moisture source might explain some  $\delta^{18}\text{O}$  variations in the Garba Guracha archive. However, because our  $^{18}\text{O}$  records

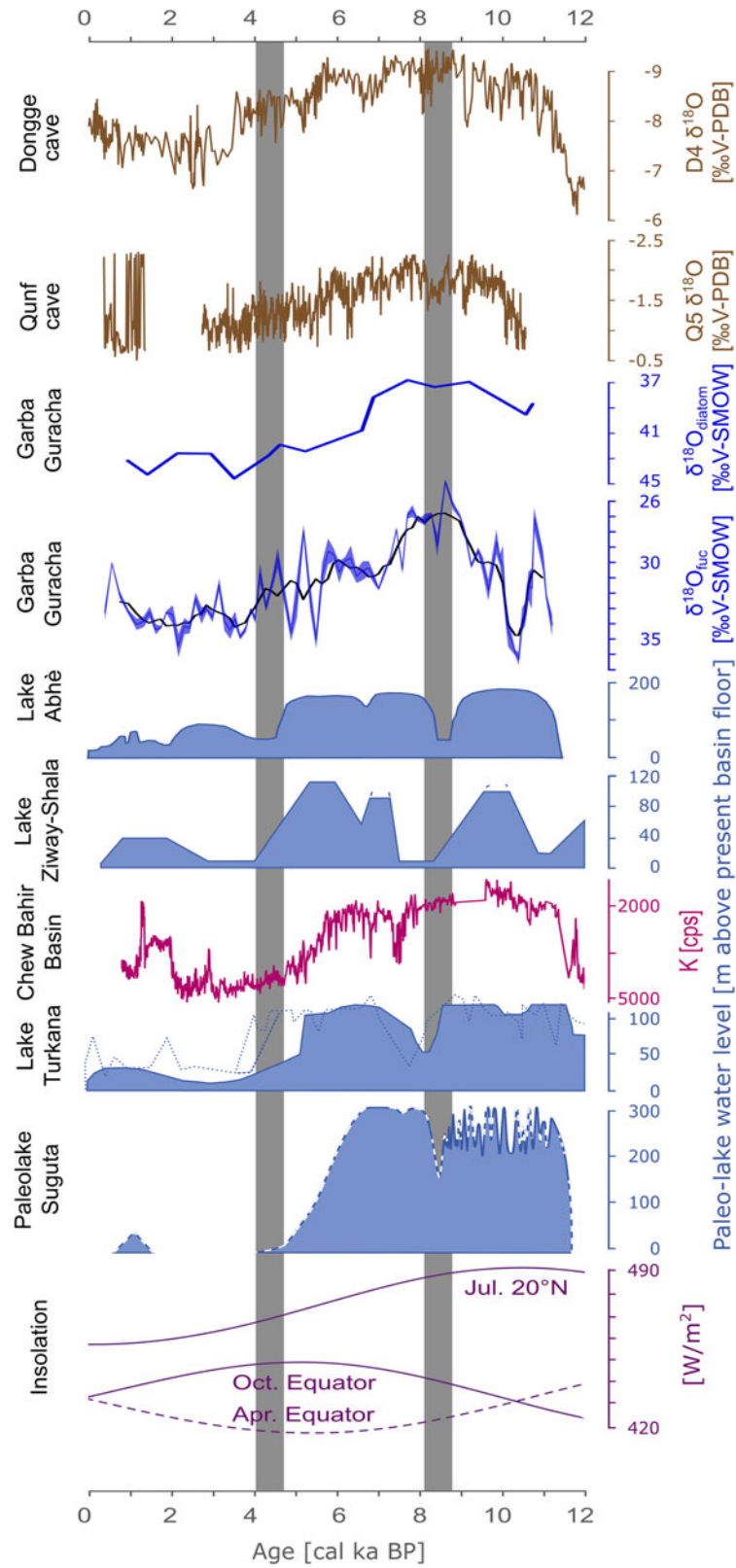


**Figure 5.** Comparison of lake level reconstructions in eastern Africa and  $\delta^{18}\text{O}$  records for the past 12,000 years (adapted from Junginger *et al.*, 2014). Dongge cave (Dykoski *et al.*, 2005), Qunf cave (Fleitmann *et al.*, 2003), Garba Guracha (this study), Lake Abhè (Gasse, 2000), Lake Ziway-Shala (Gillespie *et al.*, 1983), Chew Bahir Basin (Foerster *et al.*, 2012), Lake Turkana (Garcin *et al.*, 2012; filled curve), (Johnson *et al.*, 1991; dotted curve), (Brown and Fuller, 2008; dashed curve), Paleolake Suguta (Junginger *et al.*, 2014), and insolation variations (Laskar *et al.*, 2004).



are of aquatic origin, unlike other records, we reconstructed  $\delta^{18}\text{O}_{\text{lake water}}$ , not  $\delta^{18}\text{O}_{\text{precipitation}}$ , and suggest an additional strong influence of evaporative enrichment in the Garba Guracha record.

In open lake systems,  $\delta^{18}\text{O}_{\text{precipitation}}$  is the most crucial control on  $\delta^{18}\text{O}_{\text{lake water}}$ , whereas in closed lake systems, evaporative enrichment is the primary driver (Talbot, 1990; Lamb et al., 2002; Horton et al., 2016). Garba Guracha in modern times, with a sill level at 6 m above the sediment surface at the lake's maximum depth, is an open lake during the wet season and a closed lake system during the dry season (Supplementary Material Fig. 6). Lake water samples taken during the dry season (+ 4.7‰,  $\pm$  0.6‰; February 2017) are enriched by at least 9.2‰ compared to the annual mean  $\delta^{18}\text{O}_{\text{precipitation}}$  of -4.5‰ (Angeso station 2017; max: -1.9‰, min -6.2‰). This confirms that evaporative enrichment is able to explain a large part of the variability in the  $\delta^{18}\text{O}_{\text{fucose}}$  record (range of 11.5‰). Therefore, the reconstructed  $\delta^{18}\text{O}_{\text{lake water}}$  record of Garba Guracha likely represents changes from an open to a closed lake system and wet/dry phases, and can be interpreted in terms of precipitation-to-evaporation ratio (P/E).

### Comparison with other records

#### 11–7 cal ka BP

Our  $\delta^{18}\text{O}_{\text{fuc}}$  record suggests a high P/E at the end of the Younger Dryas, shown by values increasing to a maximum at 11 cal ka BP. This is supported by a change from organic-poor to organic-rich sedimentation, indicating a shift to favorable growth conditions for aquatic algae (Bittner et al., 2020). *Erica* expanded near the lake (Gil-Romera et al., 2019) at the onset of the Holocene (11.5–10 cal ka BP), which supports our interpretation of increased rainfall and rising P/E values. Along with such an increase, but lagged for some centuries (ca. 10.7 cal ka BP), wild-fires were triggered in the Garba Guracha catchment (Gil-Romera et al., 2019). This is possible evidence that rainfall seasonality was in place at this time, permitting dry phases favoring fire, and facilitated by enhanced biomass accumulation (Gil-Romera et al., 2019). Meyer et al. (2020) suggested a coincident wet phase (11–9.5 ka) in the Lake Chala region due to changes in the intensity of the monsoon system.

However, a maximum of  $\delta^{18}\text{O}_{\text{fuc}}$  in the Garba Guracha sediments at 10.2 cal ka BP coincides with a lake level drop in Lake Turkana (Junginger et al., 2014; Bloszies et al., 2015) and interrupts the trend towards more humid conditions (Fig. 5). Both  $\delta^{18}\text{O}_{\text{diatom}}$  and  $\delta^{18}\text{O}_{\text{fuc}}$ , but especially  $\delta^{18}\text{O}_{\text{fuc}}$ , indicate a pronounced phase of depleted  $\delta^{18}\text{O}$  values between 10 and 7 cal ka BP; suggesting a high P/E ratio due to increased rainfall amounts, a more permanent open lake phase with more constant overflow, and less evaporative enrichment. This is in agreement with the modeled overflow of Paleolake Suguta, Kenya, eastern Africa (Junginger et al., 2014) (Fig. 5). Junginger et al. (2014) suggested that the lake reached its sill level several times between 10–8.5 cal ka BP and overflowed more or less continuously from 8.5 cal ka BP until ca. 7 cal ka BP. Enhanced moisture transport into the region, indicated by reconstructed high lake levels and stronger runoff during the AHP, is well documented in the literature (Tierney et al., 2011b; Foerster et al., 2012; Tierney and deMenocal, 2013; Morrissey and Scholz, 2014; Fersi et al., 2016; Liu et al., 2017; Wagner et al., 2018; Beck et al., 2019; Jaeschke et al., 2020; Mologni et al., 2020).

A brief shift towards more positive  $\delta^{18}\text{O}$  values is present in all records coinciding with the 8.2 cal ka BP event in the northern

hemisphere, known as a short cold spell in Greenland with reduced precipitation (Dansgaard et al., 1993; Bond et al., 1997). A period of low lake levels and drought has also been reconstructed in eastern Africa for the Ziway-Shala system (Gillespie et al., 1983), Lake Malawi (Gasse et al., 2002), Lake Turkana (Garcin et al., 2012), Paleolake Suguta (Junginger et al., 2014), Lake Abhè (Gasse, 2000), and Lake Tilo (Leng et al., 1999) at that time. Thompson et al. (2002) found a maximum in wind-blown fluoride derived from dry lake basins in the Kilimanjaro ice record at ca. 8400 cal BP. However, the increase in  $\delta^{18}\text{O}_{\text{diatom}}$  and  $\delta^{18}\text{O}_{\text{fuc}}$  in Garba Guracha is rather small in comparison with the range of most regional records. This might be due to a muted precipitation change in our high-altitude archive compared to lower altitude sites or due to a temperature change rather than a precipitation decrease.

After this drought phase,  $\delta^{18}\text{O}_{\text{diatom}}$  and  $\delta^{18}\text{O}_{\text{fuc}}$  decrease again, indicating a return to humid conditions and high lake levels (Fig. 5). With the start of declining boreal summer insolation at ca. 8.7 cal ka BP, the atmospheric circulation pattern changed, and the influence of the CAB decreased in eastern Africa (Junginger et al., 2014; Wagner et al., 2018). This can be seen in our record since 7 cal ka BP when  $\delta^{18}\text{O}_{\text{diatom}}$  and  $\delta^{18}\text{O}_{\text{fuc}}$  values start to increase, indicating a shift to decreased precipitation and stronger evaporative enrichment. The phase between 10–7 cal ka BP indicates an overall increase in moisture availability concurring with the AHP.

#### 7–4 cal ka BP

Strong variability in  $\delta^{18}\text{O}_{\text{fuc}}$  from 6–4 cal ka BP coincides with the termination of the AHP. The timing of the AHP termination has been debated, and seems to be related to individual proxy responses (Castañeda et al., 2016). *Erica* and fire experienced maxima and minima during this period at Garba Guracha, but consistently decreased towards absolute minima from 5.2–2.5 cal ka BP (Gil-Romera et al., 2019), while the *Botryococcus braunii* content (Umer et al., 2007) and TOC values drop later at 4.5 cal ka BP (Bittner et al., 2020). This asynchronous proxy response may be related to the differential sensitivity of proxies to environmental change and individual drivers (Castañeda et al., 2016). Furthermore, differences in the timing of the response of various biological processes to climatic change make it difficult to assign cause and effect (e.g., perennial plants such as *Erica* may have declined, but seasonal organic matter production in the lake or transport into the lake could have continued, delaying any decline in TOC to later decades or centuries).

Despite strong variability, the mean trends in Garba Guracha  $\delta^{18}\text{O}$  values indicate a continuous transition from a humid phase before 7 cal ka BP towards a more stable arid phase after 4 cal ka BP. The more positive  $\delta^{18}\text{O}$  values after 4 cal ka BP suggest a dry climate with stronger evaporative enrichment and at least seasonally low lake levels.

In the regional context, contemporaneous decreases in lake levels have been found at north Ethiopian lakes Ziway-Shala and Abhè at ca. 4–4.5 cal ka BP (Gillespie et al., 1983; Gasse, 2000; Khalidi et al., 2020). More southern lakes, including Paleolake Suguta, Lake Turkana, and Chew Bahir, show an earlier AHP termination at ca. 5–5.5 cal ka BP (Foerster et al., 2012; Garcin et al., 2012; Junginger et al., 2014).

#### 4 cal ka BP to present

The most positive values of  $\delta^{18}\text{O}_{\text{diatom}}$  in the entire record coincide with very positive  $\delta^{18}\text{O}_{\text{fuc}}$  values at 3.5 cal ka BP, suggesting

a reduced P/E ratio and a low lake level at Garba Guracha. After 3.5 cal ka BP, the  $\delta^{18}\text{O}_{\text{diatom}}$  and  $\delta^{18}\text{O}_{\text{fuc}}$  values decrease, indicating a higher P/E ratio and increased lake level. In response to wetter conditions at 2.5 cal ka BP, an expanding heathland and more active fires may have occurred (Gil-Romera et al., 2019). However, we cannot rule out a human origin for these fires, and subsequent re-expansion of *Erica* at particular areas within the basin because anthropogenically induced changes have been detected at lower altitudes during this period (Bonnefille and Mohammed, 1994). Our findings are consistent with those of Gasse and Van Campo (1994) who found a more humid phase in eastern Africa at ca. 2.5 cal ka BP. The diatom record of Lake Ashenge also shows a humid phase between 2.5–1.5 cal ka BP (Machado et al., 1998). Moreover, a data comparison presented by Lezine et al. (2014) indicates increased humid conditions at the Horn of Africa between 3.5–1.5 cal ka BP.

During the last 1.5 cal ka BP, decreasing  $\delta^{18}\text{O}_{\text{fuc}}$  and  $\delta^{18}\text{O}_{\text{diatom}}$  values in Garba Guracha support a shift towards increased dryness at Lake Tana (documented by Marshall et al., 2011). A minimum in  $\delta^{18}\text{O}_{\text{fuc}}$  at 0.5 cal ka BP may coincide with the timing of the Little Ice Age (Grove, 2004).

## CONCLUSIONS

In eastern Africa, and especially in the Horn of Africa region, the relative scarcity of high-altitude climate proxy reconstructions inhibits understanding of regional climate change and ecosystem reaction during the Holocene and earlier. The continuous Garba Guracha archive with a high-resolution chronology allows us to present and interpret the first high-altitude (>3500 m asl)  $\delta^{18}\text{O}_{\text{fuc}}$  and  $\delta^{18}\text{O}_{\text{diatom}}$  records from the Horn of Africa. Because of the small catchment area of Garba Guracha, the sugar biomarker fucose is primarily of aquatic origin. The similar trends of  $\delta^{18}\text{O}_{\text{fuc}}$  and  $\delta^{18}\text{O}_{\text{diatom}}$  results therefore indicate that  $\delta^{18}\text{O}_{\text{fuc}}$  is a valuable proxy for  $\delta^{18}\text{O}_{\text{lake water}}$ .

Besides possible variation in the source effect, we conclude that in the case of reconstructed  $\delta^{18}\text{O}_{\text{lake water}}$  record, the effect of evaporative enrichment has to be considered to gain a better understanding of eastern African climate change. We conclude that, in general, precipitation increased at the beginning of the Holocene, leading to a primarily open lake system between ca. 10 and ca. 8 cal ka BP, with lowest  $\delta^{18}\text{O}_{\text{lake water}}$  values due to increased precipitation and reduced evaporative enrichment (lower P/E). When the lake was open and overflowing, the  $\delta^{18}\text{O}_{\text{lake water}}$  was less affected by evaporative enrichment, so the evaporative signal did not overprint the precipitation source and amount effects in the  $\delta^{18}\text{O}_{\text{lake water}}$  values.

At ca. 7 cal ka BP, a continuous shift towards drier conditions began, indicating a change towards a predominantly closed lake system. Small minima, representing phases of lower P/E, occurred at 10.8 cal ka BP, 10.2 cal ka BP, 3.5 cal ka BP, and 0.5 cal ka BP. At the temporal resolution of the Garba Guracha record, the 4.5 cal ka BP and 8.2 cal ka BP drought phases seen in eastern African lake records are not strongly imprinted in our isotope records and may point to a buffered and/or reduced response at high altitudes. Despite differences in apparent intensity, reconstructed dry and wet phases are broadly coincident with Rift Valley records, indicating similar climate controls. The Rift Valley records are influenced by eastward migration of the Congo Air Boundary, allowing Atlantic moisture to enter the region. However, the Garba Guracha record shows no evidence that the influence of Congo Basin air masses extended farther

eastwards into the Bale Mountains in the past. Further studies are needed to disentangle the source and amount effects and evaporative enrichment in stable isotope records from eastern Africa.

**Supplementary Material.** The supplementary material for this article can be found at <https://doi.org/10.1017/qua.2021.26>.

**Acknowledgments.** We are grateful to the project coordination, the Philipps University Marburg, University of Addis Ababa, the Frankfurt Zoological Society, the Ethiopian Wolf Conservation Programme, the Bale Mountains National Park, and the related staff members, especially Katinka Thielsen and Mekbib Fekadu for their logistic assistance during our fieldwork. We thank the Ethiopian Wildlife Conservation Authority for permitting our research in the Bale Mountains National Park. We thank the team of the Soil Biogeochemistry Department at Martin Luther University Halle Saale for support during lab work, in particular Marianne Benesch and Heike Maennike. We thank Dr. Miguel Sevillia-Callejo for creating the maps in Figure 1 and 2. We are grateful to two anonymous reviewers for their helpful and detailed work improving the publication.

**Author Contributions.** LB, DG, GGR, HFL, and MZ collected the samples. LB and MZ developed the concept. EL, MW, and HM analyzed and interpreted the diatom data. TB, BG, MZ, and LB analyzed and interpreted the sugar biomarker data. LB led the manuscript writing with contributions and feedback from all authors. MZ acquired the funding and supervised the work.

**Financial Support.** This research was funded by the German Research Council (DFG) in the framework of the joint Ethio-European DFG Research Unit 2358 “The Mountain Exile Hypothesis. How humans benefited from and re-shaped African high-altitude ecosystems during Quaternary climate changes.”

**Conflicts of Interest.** The authors declare that they have no conflict of interest.

## REFERENCES

- Altermatt, H.A., Neish, A.C., 1956. The biosynthesis of cell wall carbohydrates: III. Further studies on formation of cellulose and xylan from labeled monosaccharides in wheat plants. *Canadian Journal of Biochemistry and Physiology* **34**, 405–413. <https://doi.org/10.1139/o56-042>.
- Amelung, W., Cheshire, M. V., Guggenberger, G., 1996. Determination of neutral and acidic sugars in soil by capillary gas-liquid chromatography after trifluoroacetic acid hydrolysis. *Soil Biology and Biochemistry* **28**, 1631–1639. [https://doi.org/10.1016/S0038-0717\(96\)00248-9](https://doi.org/10.1016/S0038-0717(96)00248-9).
- Arnaud, F., Poulenard, J., Giguet-Covex, C., Wilhelm, B., Révillon, S., Jenny, J.-P., Revel, M., et al., 2016. Erosion under climate and human pressures: an alpine lake sediment perspective. *Quaternary Science Reviews* **152**, 1–18. <https://doi.org/10.1016/j.quascirev.2016.09.018>.
- Bailey, H.L., Henderson, A.C.G., Sloane, H.J., Snelling, A., Leng, M.J., Kaufman, D.S., 2014. The effect of species on lacustrine  $\delta^{18}\text{O}$  diatom and its implications for palaeoenvironmental reconstructions. *Journal of Quaternary Science* **29**, 393–400. <https://doi.org/10.1002/jqs.2711>.
- Bailey, H.L., Kaufman, D.S., Henderson, A.C.G., Leng, M.J., 2015. Synoptic scale controls on the  $\delta^{18}\text{O}$  in precipitation across Beringia. *Geophysical Research Letters* **42**, 4608–4616. <https://doi.org/10.1002/2015GL063983>.
- Barker, P.A., Hurrell, E.R., Leng, M.J., Wolff, C., Coquyt, C., Sloane, H.J., Verschuren, D., 2011. Seasonality in equatorial climate over the past 25 k.y. revealed by oxygen isotope records from Mount Kilimanjaro. *Geology* **39**, 1111–1114. <https://doi.org/10.1130/G32419.1>.
- Barker, P.A., Leng, M.J., Gasse, F., Huang, Y., 2007. Century-to-millennial scale climatic variability in Lake Malawi revealed by isotope records. *Earth and Planetary Science Letters* **261**, 93–103. <https://doi.org/10.1016/j.epsl.2007.06.010>.
- Barker, P.A., Street-Perrott, F.A., Leng, M.J., Greenwood, P.B., Swain, D.L., Perrott, R.A., Telford, R.J., Ficken, K.J., 2001. A 14,000-year oxygen isotope record from diatom silica in two alpine lakes on Mt. Kenya. *Science* **292**, p. 2307–2310. <https://doi.org/10.1126/science.1059612>.

- Barker, P.A., Talbot, M.R., Street-Perrott, F.A., Marret, F., Scourse, J., Odada, E.O., 2004. Late Quaternary climatic variability in intertropical Africa. In: Battarbee, R.W., Gasse, F., Stickley, C.E. (Eds.), *Past Climate Variability through Europe and Africa*. Springer Netherlands, Dordrecht, pp. 117–138. [https://doi.org/10.1007/978-1-4020-2121-3\\_7](https://doi.org/10.1007/978-1-4020-2121-3_7).
- Beck, C.C., Feibel, C.S., Wright, J.D., Mortlock, R.A., 2019. Onset of the African Humid Period by 13.9 kyr BP at Kabua Gorge, Turkana Basin, Kenya. *The Holocene* **29**, 1011–1019. <https://doi.org/10.1177/0959683619831415>.
- Berke, M.A., Johnson, T.C., Werne, J.P., Schouten, S., Sinninghe Damsté, J.S., 2012. A mid-Holocene thermal maximum at the end of the African Humid Period. *Earth and Planetary Science Letters* **351–352**, 95–104. <https://doi.org/10.1016/j.epsl.2012.07.008>.
- Bird, M.I., Haig, J., Hadeen, X., Rivera-Araya, M., Wurster, C.M., Zwart, C., 2020. Stable isotope proxy records in tropical terrestrial environments. *Palaeogeography, Palaeoclimatology, Palaeoecology* **538**, 109445. <https://doi.org/10.1016/j.palaeo.2019.109445>.
- Bittner, L., Bliedtner, M., Grady, D., Gil-Romera, G., Martin-Jones, C., Lemma, B., Mekonnen, B., et al., 2020. Revisiting afro-alpine Lake Garba Guracha in the Bale Mountains of Ethiopia: rationale, chronology, geochemistry, and paleoenvironmental implications. *Journal of Paleolimnology* **64**, 293–314. <https://doi.org/10.1007/s10933-020-00138-w>.
- Bloszies, C., Forman, S.L., Wright, D.K., 2015. Water level history for Lake Turkana, Kenya in the past 15,000 years and a variable transition from the African Humid Period to Holocene aridity. *Global and Planetary Change* **132**, 64–76. <https://doi.org/10.1016/j.gloplacha.2015.06.006>.
- Bond, G., Showers, W., Cheseby, M., Lotti, R., Almasi, P., deMenocal, P., Priore, P., Cullen, H., Hajdas, I., Bonani, G., 1997. A pervasive millennial-scale cycle in North Atlantic Holocene and glacial climates. *Science* **278**, 1257–1266. <https://doi.org/10.1126/science.278.5341.1257>.
- Bonnefille, R., Mohammed, U., 1994. Pollen-inferred climatic fluctuations in Ethiopia during the last 3000 years. *Palaeogeography, Palaeoclimatology, Palaeoecology* **109**, 331–343. [https://doi.org/10.1016/0031-0182\(94\)90183-X](https://doi.org/10.1016/0031-0182(94)90183-X).
- Brandriss, M.E., O'Neil, J.R., Edlund, M.B., Stoermer, E.F., 1998. Oxygen isotope fractionation between diatomaceous silica and water. *Geochimica et Cosmochimica Acta* **62**, 1119–1125. [https://doi.org/10.1016/S0016-7037\(98\)00054-4](https://doi.org/10.1016/S0016-7037(98)00054-4).
- Brown, F.H., Fuller, C.R., 2008. Stratigraphy and tephra of the Kibish Formation, southwestern Ethiopia. *Journal of Human Evolution* **55**, 366–403. <https://doi.org/10.1016/j.jhevol.2008.05.009>.
- Burget, E.G., Verma, R., Molhøj, M., Reiter, W.-D., 2003. The biosynthesis of l-arabinose in plants: molecular cloning and characterization of a Golgi-localized UDP-d-xylose 4-epimerase encoded by the MUR4 gene of *Arabidopsis*. *The Plant Cell* **15**, 523–531. <https://doi.org/10.1105/tpc.008425>.
- Camberlin, P., 1997. Rainfall anomalies in the source region of the Nile and their connection with the Indian Summer Monsoon. *Journal of Climate* **10**, 1380–1392. [https://doi.org/10.1175/1520-0442\(1997\)010<1380:RAITSR>2.0.CO;2](https://doi.org/10.1175/1520-0442(1997)010<1380:RAITSR>2.0.CO;2).
- Cartier, R., Sylvestre, F., Paillès, C., Sonzogni, C., Couapel, M., Alexandre, A., Mazur, J.-C., Brisset, E., Miramont, C., Guiter, F., 2019. Diatom-oxygen isotope record from high-altitude Lake Petit (2200ma.s.l.) in the Mediterranean Alps: shedding light on a climatic pulse at 4.2 ka. *Climate of the Past* **15**, 253–263. <https://doi.org/10.5194/cp-15-253-2019>.
- Castañeda, I.S., Schouten, S., Pätzold, J., Lucassen, F., Kasemann, S., Kuhlmann, H., Schefuß, E., 2016. Hydroclimate variability in the Nile River Basin during the past 28,000 years. *Earth and Planetary Science Letters* **438**, 47–56. <https://doi.org/10.1016/j.epsl.2015.12.014>.
- Catalan, J., Camarero, L., Felip, M., Pla, S., Ventura, M., Buchaca, T., Bartumeus, F., et al., 2006. High mountain lakes: extreme habitats and witnesses of environmental changes. *Limnetica* **25**, 551–584.
- Catalan, J., Pla-Rabés, S., Wolfe, A.P., Smol, J.P., Rühland, K.M., Anderson, N.J., Kopáček, J., et al., 2013. Global change revealed by palaeolimnological records from remote lakes: a review. *Journal of Paleolimnology* **49**, 513–535. <https://doi.org/10.1007/s10933-013-9681-2>.
- Chapligin, B., Leng, M.J., Webb, E., Alexandre, A., Dodd, J.P., Ijiri, A., Lücke, A., et al., 2011. Inter-laboratory comparison of oxygen isotope compositions from biogenic silica. *Geochimica et Cosmochimica Acta* **75**, 7242–7256. <https://doi.org/https://doi.org/10.1016/j.gca.2011.08.011>.
- Chapligin, B., Meyer, H., Bryan, A., Snyder, J., Kemnitz, H., 2012. Assessment of purification and contamination correction methods for analysing the oxygen isotope composition from biogenic silica. *Chemical Geology* **300–301**, 185–199. <https://doi.org/10.1016/j.chemgeo.2012.01.004>.
- Chapligin, B., Meyer, H., Friedrichsen, H., Marent, A., Sohns, E., Hubberten, H.-W., 2010. A high-performance, safer and semi-automated approach for the  $\delta^{18}\text{O}$  analysis of diatom silica and new methods for removing exchangeable oxygen. *Rapid Communications in Mass Spectrometry* **24**, 2655–2664. <https://doi.org/10.1002/rcm.4689>.
- Clayton, R.N., Mayeda, T.K., 1963. The use of bromine pentafluoride in the extraction of oxygen from oxides and silicates for isotopic analysis. *Geochimica et Cosmochimica Acta* **27**, 43–52. [https://doi.org/10.1016/0016-7037\(63\)90071-1](https://doi.org/10.1016/0016-7037(63)90071-1).
- Cole, J.E., Rind, D., Webb, R.S., Jouzel, J., Healy, R., 1999. Climatic controls on interannual variability of precipitation  $\delta^{18}\text{O}$ : simulated influence of temperature, precipitation amount, and vapor source region. *Journal of Geophysical Research: Atmospheres* **104**, 14,223–14,235. <https://doi.org/10.1029/1999JD900182>.
- Collins, J.A., Prange, M., Caley, T., Gimeno, L., Beckmann, B., Mulitza, S., Skonieczny, C., Roche, D., Schefuß, E., 2017. Rapid termination of the African Humid Period triggered by northern high-latitude cooling. *Nature Communications* **8**, 1372. <https://doi.org/10.1038/s41467-017-01454-y>.
- Costa, K., Russell, J., Konecky, B., Lamb, H., 2014. Isotopic reconstruction of the African Humid Period and Congo Air Boundary migration at Lake Tana, Ethiopia. *Quaternary Science Reviews* **83**, 58–67. <https://doi.org/10.1016/j.quascirev.2013.10.031>.
- Crespin, J., Sylvestre, F., Alexandre, A., Sonzogni, C., Paillès, C., Perga, M.-E., 2010. Re-examination of the temperature-dependent relationship between  $\delta^{18}\text{O}$  diatoms and  $\delta^{18}\text{O}$  lakewater and implications for paleoclimate inferences. *Journal of Paleolimnology* **44**, 547–557. <https://doi.org/10.1007/s10933-010-9436-2>.
- Dansgaard, W., 1964. Stable isotopes in precipitation. *Tellus* **16**, 436–468.
- Dansgaard, W., Johnsen, S.J., Clausen, H.B., Dahl-Jensen, D., Gundestrup, N.S., Hammer, C.U., Hvidberg, C.S., et al., 1993. Evidence for general instability of past climate from a 250-kyr ice-core record. *Nature* **364**, 218–220. <https://doi.org/10.1038/364218a0>.
- Davies, T.D., Vincent, C.E., Beresford, A.K.C., 1985. July–August rainfall in west-central Kenya. *Journal of Climatology* **5**, 17–33. <https://doi.org/10.1002/joc.3370050103>.
- deMenocal, P., Ortiz, J., Guilderson, T., Adkins, J., Sarnthein, M., Baker, L., Yarusinsky, M., 2000. Abrupt onset and termination of the African Humid Period: Quaternary Science Reviews **19**, 347–361. [https://doi.org/10.1016/S0277-3791\(99\)00081-5](https://doi.org/10.1016/S0277-3791(99)00081-5).
- Dodd, J.P., Sharp, Z.D., 2010. A laser fluorination method for oxygen isotope analysis of biogenic silica and a new oxygen isotope calibration of modern diatoms in freshwater environments. *Geochimica et Cosmochimica Acta* **74**, 1381–1390. <https://doi.org/10.1016/j.gca.2009.11.023>.
- Dodd, J.P., Sharp, Z.D., Fawcett, P.J., Brearley, A.J., McCubbin, F.M., 2012. Rapid post-mortem maturation of diatom silica oxygen isotope values. *Geochemistry, Geophysics, Geosystems* **13**, Q09014. <https://doi.org/10.1029/2011GC004019>.
- Dykoski, C.A., Edwards, R.L., Cheng, H., Yuan, D., Cai, Y., Zhang, M., Lin, Y., Qing, J., An, Z., Revenaugh, J., 2005. A high-resolution, absolute-dated Holocene and deglacial Asian monsoon record from Dongge Cave, China. *Earth and Planetary Science Letters* **233**, 71–86. <https://doi.org/10.1016/j.epsl.2005.01.036>.
- Fersi, W., Lézine, A.-M., Bassinot, F., 2016. Hydro-climate changes over southwestern Arabia and the Horn of Africa during the last glacial–interglacial transition: a pollen record from the Gulf of Aden. *Review of Palaeobotany and Palynology* **233**, 176–185. <https://doi.org/10.1016/j.revpalbo.2016.04.002>.
- Finney, D.L., Marsham, J.H., Walker, D.P., Birch, C.E., Woodhams, B.J., Jackson, L.S., Hardy, S., 2020. The effect of westerlies on East African rainfall and the associated role of tropical cyclones and the Madden-Julian Oscillation. *Quarterly Journal of the Royal Meteorological Society* **146**, 647–664. <https://doi.org/10.1002/qj.3698>.

- Fleitmann, D., Burns, S.J., Neff, U., Mangini, A., Matter, A., 2003. Changing moisture sources over the last 330,000 years in northern Oman from fluid-inclusion evidence in speleothems. *Quaternary Research* **60**, 223–232. [https://doi.org/10.1016/S0033-5894\(03\)00086-3](https://doi.org/10.1016/S0033-5894(03)00086-3).
- Foerster, V., Junginger, A., Langkamp, O., Gebru, T., Asrat, A., Umer, M., Lamb, H.F., et al., 2012. Climatic change recorded in the sediments of the Chew Bahir Basin, southern Ethiopia, during the last 45,000 years. *Quaternary International* **274**, 25–37. <https://doi.org/10.1016/j.quaint.2012.06.028>.
- Garcin, Y., Melnick, D., Strecker, M.R., Olago, D., Tiercelin, J.-J., 2012. East African mid-Holocene wet–dry transition recorded in palaeo-shorelines of Lake Turkana, northern Kenya Rift. *Earth and Planetary Science Letters* **331–332**, 322–334. <https://doi.org/10.1016/j.epsl.2012.03.016>.
- Gasse, F., 2000. Hydrological changes in the African tropics since the Last Glacial Maximum. *Quaternary Science Reviews* **19**, 189–211. [https://doi.org/10.1016/S0277-3791\(99\)00061-X](https://doi.org/10.1016/S0277-3791(99)00061-X).
- Gasse, F., Barker, P., Johnson, T.C., 2002. A 24,000 yr Diatom Record from the Northern Basin of Lake Malawi. In: Odada, E.O., Olago, D.O. (Eds.), *The East African Great Lakes: limnology, palaeolimnology and biodiversity*. Springer Netherlands, Dordrecht, pp. 393–414. [https://doi.org/10.1007/0-306-48201-0\\_16](https://doi.org/10.1007/0-306-48201-0_16).
- Gasse, F., Van Campo, E., 1994. Abrupt post-glacial climate events in West Asia and North Africa monsoon domains. *Earth and Planetary Science Letters* **126**, 435–456. [https://doi.org/10.1016/0012-821X\(94\)90123-6](https://doi.org/10.1016/0012-821X(94)90123-6).
- Gil-Romera, G., Adolf, C., Benito Blas, M., Bittner, L., Johansson, M.M.U., Grady, D.D.A., Lamb, H.H.F., et al., 2019. Long-term fire resilience of the Ericaceous Belt, Bale Mountains, Ethiopia. *Biology Letters* **15**, 20190357. <https://doi.org/10.1098/rsbl.2019.0357>.
- Gillespie, R., Street-Perrott, F.A., Switsur, R., 1983. Post-glacial arid episodes in Ethiopia have implications for climate prediction. *Nature* **306**, 680–683. <https://doi.org/10.1038/306680a0>.
- Groos, A., Akçar, N., Yesilyurt, S., Mieke, G., Vockenhuber, C., Veit, H., 2021. Nonuniform Late Pleistocene glacier fluctuations in tropical Eastern Africa. *Science Advances* **7**, eabb6826. <https://doi.org/10.1126/sciadv.abb6826>.
- Groos, A.R., Niederhauser, J., Wraase, L., Hänsel, F., Naus, T., Akçar, N., Veit, H., 2020. Implications of present ground temperatures and relict stone stripes in the Ethiopian Highlands for the palaeoclimate of the tropics. *Earth Surface Dynamics Discussions* **2020**, 1–37. <https://doi.org/10.5194/esurf-2020-53>.
- Grove, J.M., 2004. *Little Ice Ages*, 2nd ed. Routledge, London. <https://doi.org/10.4324/9780203770269>
- Harper, A.D., Bar-Peled, M., 2002. Biosynthesis of UDP-xylose. Cloning and characterization of a novel *Arabidopsis* gene family, UXS, encoding soluble and putative membrane-bound UDP-glucuronic acid decarboxylase isoforms. *Plant Physiology* **130**, 2188–2198. <https://doi.org/10.1104/pp.009654>.
- Hepp, J., Glaser, B., Juchelka, D., Mayr, C., Rozanski, K., Schäfer, I.K., Stöckli, W., Tuthorn, M., Zech, R., Zech, M., 2019. Validation of a coupled  $\delta^2\text{H}_{\text{n-alkane}}-\delta^{18}\text{O}_{\text{sugar}}$  paleohygrometer approach based on a climate chamber experiment. *Biogeosciences Discussion* **2019**, 1–30. <https://doi.org/10.5194/bg-2019-427>.
- Hepp, J., Rabus, M., Anhäuser, T., Bromm, T., Laforsch, C., Sirocko, F., Glaser, B., Zech, M., 2016. A sugar biomarker proxy for assessing terrestrial versus aquatic sedimentary input. *Organic Geochemistry* **98**, 98–104. <https://doi.org/10.1016/j.orggeochem.2016.05.012>.
- Hepp, J., Tuthorn, M., Zech, R., Mügler, I., Schlütz, F., Zech, W., Zech, M., 2015. Reconstructing lake evaporation history and the isotopic composition of precipitation by a coupled  $\delta^{18}\text{O}-\delta^2\text{H}$  biomarker approach. *Journal of Hydrology* **529**, 622–631. <https://doi.org/10.1016/j.jhydrol.2014.10.012>.
- Hepp, J., Zech, R., Rozanski, K., Tuthorn, M., Glaser, B., Greule, M., Keppler, F., Huang, Y., Zech, W., Zech, M., 2017. Late Quaternary relative humidity changes from Mt. Kilimanjaro, based on a coupled  $^2\text{H}-^{18}\text{O}$  biomarker paleohygrometer approach. *Quaternary International* **438**, 116–130. <https://doi.org/10.1016/j.quaint.2017.03.059>.
- Hillman, J., 1986. Conservation in Bale Mountains National Park, Ethiopia. *Oryx* **20**, 89–94. <https://doi.org/10.1017/S0030605300026314>.
- Hillman, J., 1988. The Bale Mountains National Park area, southeast Ethiopia, and its management. *Mountain Research and Development* **8**, 253–258. <https://doi.org/10.2307/3673456>.
- Hills, R.C., 1979. The Structure of the Inter-Tropical Convergence Zone in equatorial Africa and its relationship to East African Rainfall. *Transactions of the Institute of British Geographers* **4**, 329–352. <https://doi.org/10.2307/622055>.
- Horton, T.W., Defliese, W.F., Tripathi, A.K., Oze, C., 2016. Evaporation induced  $^{18}\text{O}$  and  $^{13}\text{C}$  enrichment in lake systems: a global perspective on hydrologic balance effects. *Quaternary Science Reviews* **131**, 365–379. <https://doi.org/10.1016/j.quascirev.2015.06.030>.
- Jaeschke, A., Thienemann, M., Schefuß, E., Urban, J., Schäbitz, F., Wagner, B., Rethemeyer, J., 2020. Holocene hydroclimate variability and vegetation response in the Ethiopian Highlands (Lake Dendi). *Frontiers in Earth Science* **8**, 585770. <https://doi.org/10.3389/feart.2020.585770>.
- Johnson, T.C., Halfman, J.D., Showers, W.J., 1991. Paleoclimate of the past 4000 years at Lake Turkana, Kenya, based on the isotopic composition of authigenic calcite. *Palaeogeography, Palaeoclimatology, Palaeoecology* **85**, 189–198. [https://doi.org/10.1016/0031-0182\(91\)90158-N](https://doi.org/10.1016/0031-0182(91)90158-N).
- Junginger, A., Roller, S., Olaka, L.A., Trauth, M.H., 2014. The effects of solar irradiation changes on the migration of the Congo Air Boundary and water levels of paleo-Lake Suguta, Northern Kenya Rift, during the African Humid Period (15–5 ka BP) CA. *Palaeogeography, Palaeoclimatology, Palaeoecology* **396**, 1–16. <https://doi.org/10.1016/j.palaeo.2013.12.007>.
- Khalidi, L., Mologni, C., Ménard, C., Coudert, L., Gabriele, M., Davtian, G., Cauliez, J., et al., 2020. 9000 years of human lakeside adaptation in the Ethiopian Afar: fisher-foragers and the first pastoralists in the Lake Abhe basin during the African Humid Period. *Quaternary Science Reviews* **243**, 106459. <https://doi.org/https://doi.org/10.1016/j.quascirev.2020.106459>.
- Kidane, Y., Stahlmann, R., Beierkuhnlein, C., 2012. Vegetation dynamics, and land use and land cover change in the Bale Mountains, Ethiopia. *Environmental Monitoring and Assessment* **184**, p. 7473–7489. <https://doi.org/10.1007/s10661-011-2514-8>.
- Knapp, D.R., 1979. *Handbook of Analytical Derivatization Reactions*. John Wiley & Sons, New York, Chichester, Brisbane, Toronto, Singapore.
- Kostrova, S.S., Meyer, H., Bailey, H.L., Ludikova, A.V., Gromig, R., Kuhn, G., Shibaev, Y.A., Kozachek, A.V., Ekaykin, A.A., Chaplignin, B., 2019. Holocene hydrological variability of Lake Ladoga, northwest Russia, as inferred from diatom oxygen isotopes. *Boreas* **48**, 361–376. <https://doi.org/10.1111/bor.12385>.
- Kostrova, S.S., Meyer, H., Chaplignin, B., Tarasov, P.E., Bezrukova, E.V., 2014. The last glacial maximum and late glacial environmental and climate dynamics in the Baikal region inferred from an oxygen isotope record of lacustrine diatom silica. *Quaternary International* **348**, 25–36. <https://doi.org/10.1016/j.quaint.2014.07.034>.
- Labeyrie, L., 1974. New approach to surface seawater palaeotemperatures using  $^{18}\text{O}/^{16}\text{O}$  ratios in silica of diatom frustules. *Nature* **248**, 40–42. <https://doi.org/10.1038/248040a0>.
- Lamb, A., Leng, M., Sloane, H., Telford, R., 2005. A comparison of the palaeoclimate signals from diatom oxygen isotope ratios and carbonate oxygen isotope ratios from a low latitude crater lake. *Palaeogeography, Palaeoclimatology, Palaeoecology* **223**, 290–302. <https://doi.org/10.1016/j.palaeo.2005.04.011>.
- Lamb, H.F., Kebede, S., Leng, M.J., Ricketts, D., Telford, R.J., Umer, M., 2002. Origin and Isotopic Composition of Aragonite Laminae in an Ethiopian Crater Lake. In: Odada E.O., Olago D.O. (Eds.), *The East African Great Lakes: Limnology, Palaeolimnology and Biodiversity*. Kluwer, Dordrecht, The Netherlands, pp. 487–508.
- Laskar, J., Robutel, P., Joutel, F., Gastineau, M., Correia, A.C.M., Levrard, B., 2004. A long-term numerical solution for the insolation quantities of the Earth. *Astronomy & Astrophysics* **428**, 261–285. <https://doi.org/10.1051/0004-6361:20041335>.
- Leclerc, A.J., Labeyrie, L., 1987. Temperature dependence of the oxygen isotopic fractionation between diatom silica and water. *Earth and Planetary Science Letters* **84**, 69–74. [https://doi.org/10.1016/0012-821X\(87\)90177-4](https://doi.org/10.1016/0012-821X(87)90177-4).
- Lemma, B., Kebede Gurmessa, S., Nemomissa, S., Otte, I., Glaser, B., Zech, M., 2020. Spatial and temporal  $^2\text{H}$  and  $^{18}\text{O}$  isotope variation of contemporary precipitation in the Bale Mountains, Ethiopia. *Isotopes in Environmental and Health Studies* **56**, 122–135. <https://doi.org/10.1080/10256016.2020.1717487>.
- Leng, M., Barnker, P., Greenwood, P., Roberts, N., Reed, J., 2001. Oxygen isotope analysis of diatom silica and authigenic calcite from Lake

- Pinarbasi, Turkey. *Journal of Paleolimnology* 25, 343–349. <https://doi.org/10.1023/A:1011169832093>.
- Leng, M.J., Barker, P.A., 2006. A review of the oxygen isotope composition of lacustrine diatom silica for palaeoclimate reconstruction. *Earth-Science Reviews* 75, 5–27. <https://doi.org/https://doi.org/10.1016/j.earscirev.2005.10.001>
- Leng, M.J., Lamb, A.L., Lamb, H.F., Telford, R.J., 1999. Palaeoclimatic implications of isotopic data from modern and early Holocene shells of the freshwater snail *Melanoides tuberculata*, from lakes in the Ethiopian Rift Valley. *Journal of Paleolimnology* 21, 97–106. <https://doi.org/10.1023/A:1008079219280>.
- Leng, M.J., Metcalfe, S.E., Davies, S.J., 2005. Investigating late Holocene climate variability in central Mexico using carbon isotope ratios in organic materials and oxygen isotope ratios from diatom silica within lacustrine sediments. *Journal of Paleolimnology* 34, 413–431. <https://doi.org/10.1007/s10933-005-6748-8>.
- Levin, N.E., Zipsper, E.J., Ceding, T.E., 2009. Isotopic composition of waters from Ethiopia and Kenya: Insights into moisture sources for eastern Africa. *Journal of Geophysical Research Atmospheres* 114, D23306. <https://doi.org/10.1029/2009JD012166>
- Lezine, A.-M., Bassinot, F., Peterschmitt, J.-Y., 2014. Orbitally-induced changes of the Atlantic and Indian monsoons over the past 20,000 years: new insights based on the comparison of continental and marine records. *Bulletin de la Société Géologique de France* 185, 3–12. <https://doi.org/10.2113/gssgobull.185.1.3>.
- Liu, X., Rendle-Bühning, R., Kuhlmann, H., Li, A., 2017. Two phases of the Holocene East African Humid Period: Inferred from a high-resolution geochemical record off Tanzania. *Earth and Planetary Science Letters* 460, 123–134. <https://doi.org/10.1016/j.epsl.2016.12.016>.
- Löffler, H., 1978. Limnology and paleolimnological data on the Bale Mountain Lakes. Verh. International Verein. *Limnology* 20, 1131–1138.
- Loomis, S.E., Russell, J.M., Lamb, H.F., 2015. Northeast African temperature variability since the late Pleistocene. *Palaeogeography, Palaeoclimatology, Palaeoecology* 423, 80–90. <https://doi.org/10.1016/j.palaeo.2015.02.005>.
- Loomis, S.E., Russell, J.M., Verschuren, D., Morrill, C., De Cort, G., Sinninghe Damsté, J.S., Olago, D., Eggermont, H., Street-Perrott, F.A., Kelly, M.A., 2017. The tropical lapse rate steepened during the Last Glacial Maximum. *Science Advances* 3, e1600815. <https://doi.org/10.1126/sciadv.1600815>.
- Machado, M.J., Pérez-González, A., Benito, G., 1998. Paleoenvironmental Changes during the Last 4000 yr in the Tigray, northern Ethiopia. *Quaternary Research* 49, 312–321. <https://doi.org/10.1006/qres.1998.1965>.
- Mackay, A.W., Swann, G.E.A., Fagel, N., Fietz, S., Leng, M.J., Morley, D., Rioual, P., Tarasov, P., 2013. Hydrological instability during the Last Interglacial in central Asia: a new diatom oxygen isotope record from Lake Baikal. *Quaternary Science Reviews* 66, 45–54. <https://doi.org/10.1016/j.quascirev.2012.09.025>.
- Marshall, M.H., Lamb, H.F., Huws, D., Davies, S.J., Bates, R., Bloemendal, J., Boyle, J., Leng, M.J., Umer, M., Bryant, C., 2011. Late Pleistocene and Holocene drought events at Lake Tana, the source of the Blue Nile. *Global and Planetary Change* 78, 147–161. <https://doi.org/10.1016/j.gloplacha.2011.06.004>.
- Marshall, M., Lamb, H., Davies, S., Leng, M., Bedaso, Z., Umer, M., Bryant, C., 2009. Climatic change in northern Ethiopia during the past 17,000 years: a diatom and stable isotope record from Lake Ashenge. *Palaeogeography, Palaeoclimatology, Palaeoecology* 279, p. 114–127. <https://doi.org/10.1016/j.palaeo.2009.05.003>.
- Mayr, C., Laprida, C., Lücke, A., Martín, R.S., Massafèrro, J., Ramón-Mercu, J., Wissel, H., 2015. Oxygen isotope ratios of chironomids, aquatic macrophytes and ostracods for lake-water isotopic reconstructions—results of a calibration study in Patagonia. *Journal of Hydrology* 529, 600–607. <https://doi.org/10.1016/j.jhydrol.2014.11.001>.
- Meyer, H., Chaplignin, B., Hoff, U., Nazarova, L., Diekmann, B., 2015. Oxygen isotope composition of diatoms as late Holocene climate proxy at Two-Yurts Lake, Central Kamchatka, Russia. *Global and Planetary Change* 134, 118–128. <https://doi.org/10.1016/j.gloplacha.2014.04.008>.
- Meyer, I., Van Daele, M., Tanghe, N., De Batist, M., Verschuren, D., 2020. Reconstructing East African monsoon variability from grain-size distributions: end-member modeling and source attribution of diatom-rich sediments from Lake Chala. *Quaternary Science Reviews* 247, 106574. <https://doi.org/10.1016/j.quascirev.2020.106574>.
- Miehe, S., Miehe, G., 1994. *Ericaceous Forests and Heathlands in the Bale Mountains of South Ethiopia: Ecology and Man's Impact*. T. Warnke Verlag, Hamburg.
- Mologni, C., Revel, M., Blanchet, C., Bosch, D., Develle, A.-L., Orange, F., Luc, B., Khalidi, L., Ducassou, E., Migeon, S., 2020. Frequency of exceptional Nile flood events as an indicator of Holocene hydro-climatic changes in the Ethiopian Highlands. *Quaternary Science Reviews* 247, 106543. <https://doi.org/10.1016/j.quascirev.2020.106543>.
- Morley, D.W., Leng, M.J., Mackay, A.W., Sloane, H.J., 2005. Late glacial and Holocene environmental change in the Lake Baikal region documented by oxygen isotopes from diatom silica. *Global and Planetary Change* 46, 221–233. <https://doi.org/10.1016/j.gloplacha.2004.09.018>.
- Morrissey, A., Scholz, C.A., 2014. Paleohydrology of Lake Turkana and its influence on the Nile River system. *Palaeogeography, Palaeoclimatology, Palaeoecology* 403, 88–100. <https://doi.org/10.1016/j.palaeo.2014.03.029>.
- Moschen, R., Lücke, A., Schleser, G.H., 2005. Sensitivity of biogenic silica oxygen isotopes to changes in surface water temperature and palaeoclimatology. *Geophysical Research Letters* 32, L07708. <https://doi.org/10.1029/2004GL022167>.
- Nakamura, K., 1968. Equatorial westerlies over East Africa and their climatological significance. *Geographical Review of Japan* 41, 359–373. <https://doi.org/10.4157/grj.41.359>.
- Narancic, B., Pienitz, R., Chaplignin, B., Meyer, H., Francus, P., Guilbault, J.-P., 2016. Postglacial environmental succession of Nettiing Lake (Baffin Island, Canadian Arctic) inferred from biogeochemical and microfossil proxies. *Quaternary Science Reviews* 147, 391–405. <https://doi.org/10.1016/j.quascirev.2015.12.022>.
- Ogier, S., Disnar, J.-R., Albéric, P., Bourdier, G., 2001. Neutral carbohydrate geochemistry of particulate material (trap and core sediments) in an eutrophic lake (Aydat, France). *Organic Geochemistry* 32, 151–162. [https://doi.org/10.1016/S0146-6380\(00\)00138-8](https://doi.org/10.1016/S0146-6380(00)00138-8).
- Osmaston, H.A., Mitchell, W.A., Osmaston, J.A.N., 2005. Quaternary glaciation of the Bale Mountains, Ethiopia. *Journal of Quaternary Science* 20, 593–606. <https://doi.org/10.1002/jqs.931>.
- Ossendorf, G., Groos, A., Bromm, T., Girma Tekelemariam, M., Glaser, B., Lesur, J., Schmidt, J., et al., 2019. Middle Stone Age foragers resided in high elevations of the glaciated Bale Mountains, Ethiopia. *Science* 365, 583–587.
- Polissar, P.J., Abbott, M.B., Shemesh, A., Wolfe, A.P., Bradley, R.S., 2006. Holocene hydrologic balance of tropical South America from oxygen isotopes of lake sediment opal, Venezuelan Andes. *Earth and Planetary Science Letters* 242, 375–389. <https://doi.org/10.1016/j.epsl.2005.12.024>.
- Rosqvist, G., Jonsson, C., Yam, R., Karlén, W., Shemesh, A., 2004. Diatom oxygen isotopes in pro-glacial lake sediments from northern Sweden: a 5000 year record of atmospheric circulation. *Quaternary Science Reviews* 23, 851–859. <https://doi.org/10.1016/j.quascirev.2003.06.009>.
- Rozanski, K., Araguás-Araguás, L., Gonfiantini, R., 1993. Isotopic Patterns in Modern Global Precipitation. In: Swart, P.K., Lohmann, K.C., Mckenzie, J., Savin, S. (Eds.), *Climate Change in Continental Isotopic Records*. *Geophysical Monograph Series* 78, p. 1–36. <https://doi.org/doi:10.1029/GM078p001>.
- Schiff, C.J., Kaufman, D.S., Wolfe, A.P., Dodd, J., Sharp, Z., 2009. Late Holocene storm-trajectory changes inferred from the oxygen isotope composition of lake diatoms, south Alaska. *Journal of Paleolimnology* 41, 189–208. <https://doi.org/10.1007/s10933-008-9261-z>.
- Schmidt, M., Botz, R., Rickert, D., Bohrmann, G., Hall, S.R., Mann, S., 2001. Oxygen isotopes of marine diatoms and relations to opal-A maturation. *Geochimica et Cosmochimica Acta* 65, 201–211. [https://doi.org/10.1016/S0016-7037\(00\)00534-2](https://doi.org/10.1016/S0016-7037(00)00534-2).
- Sharp, Z., 2017. *Principles of Stable Isotope Geochemistry, 2nd Edition*. University of New Mexico, Digital Repository. <https://doi.org/10.5072/FK2GB24S9F>.
- Street-Perrott, F.A., Barker, P.A., Leng, M.J., Sloane, H.J., Wooller, M.J., Ficken, K.J., Swain, D.L., 2008. Towards an understanding of late Quaternary variations in the continental biogeochemical cycle of silicon: multi-isotope and sediment-flux data for Lake Rutundu, Mt Kenya, East Africa, since 38 ka BP. *Journal of Quaternary Science* 23, 375–387. <https://doi.org/10.1002/jqs.1187>.

- Talbot, M.R., 1990. A review of the palaeohydrological interpretation of carbon and oxygen isotopic ratios in primary lacustrine carbonates. *Chemical Geology: Isotope Geoscience section* **80**, 261–279. [https://doi.org/10.1016/0168-9622\(90\)90009-2](https://doi.org/10.1016/0168-9622(90)90009-2).
- Thompson, L.G., Mosley-Thompson, E., Davis, M.E., Henderson, K.A., Brecher, H.H., Zagorodnov, V.S., Mashiotta, T.A., et al., 2002. Kilimanjaro ice core records: evidence of Holocene climate change in tropical Africa. *Science* **298**, 589–593. <https://doi.org/10.1126/science.1073198>.
- Tiercelin, J.J., Gibert, E., Umer, M., Bonnefille, R., Disnar, J.R., Lézine, A.M., Hureau-Mazaudier, D., Travi, Y., Keravis, D., Lamb, H.F., 2008. High-resolution sedimentary record of the last deglaciation from a high-altitude lake in Ethiopia. *Quaternary Science Reviews* **27**, 449–467. <https://doi.org/10.1016/j.quascirev.2007.11.002>.
- Tierney, J.E., deMenocal, P.B., 2013. Abrupt shifts in Horn of Africa hydroclimate since the Last Glacial Maximum. *Science* **342**, 843–846. <https://doi.org/10.1126/science.1240411>.
- Tierney, J.E., Lewis, S.C., Cook, B.I., LeGrande, A.N., Schmidt, G.A., 2011a. Model, proxy and isotopic perspectives on the East African Humid Period. *Earth and Planetary Science Letters* **307**, 103–112. <https://doi.org/10.1016/j.epsl.2011.04.038>.
- Tierney, J.E., Russell, J.M., Sinninghe Damsté, J.S., Huang, Y., Verschuren, D., 2011b. Late Quaternary behavior of the East African monsoon and the importance of the Congo Air Boundary. *Quaternary Science Reviews* **30**, 798–807. <https://doi.org/10.1016/j.quascirev.2011.01.017>.
- Tyler, J.J., Sloane, H.J., Rickaby, R.E.M., Cox, E.J., Leng, M.J., 2017. Post-mortem oxygen isotope exchange within cultured diatom silica. *Rapid Communications in Mass Spectrometry* **31**, 1749–1760. <https://doi.org/10.1002/rcm.7954>.
- Uhlig, S.K., 1988. Mountain Forests and the Upper Tree Limit on the Southeastern Plateau of Ethiopia. *Mountain Research and Development* **8**, 227–234. <https://doi.org/10.2307/3673452>.
- Uhlig, S.K., Uhlig, K., 1991. Studies on the Altitudinal Zonation of Forests and Alpine Plants in the Central Bale Mountains, Ethiopia. *Mountain Research and Development* **11**, 153–156. <https://doi.org/10.2307/3673574>.
- Umer, M., Lamb, H.F., Bonnefille, R., Lézine, A.M., Tiercelin, J.J., Gibert, E., Cazet, J.P., Watrin, J., 2007. Late Pleistocene and Holocene vegetation history of the Bale Mountains, Ethiopia. *Quaternary Science Reviews* **26**, 2229–2246. <https://doi.org/10.1016/j.quascirev.2007.05.004>.
- van der Lubbe, H.J.L., Krause-Nehring, J., Junginger, A., Garcin, Y., Joordens, J.C.A., Davies, G.R., Beck, C., Feibel, C.S., Johnson, T.C., Vonhof, H.B., 2017. Gradual or abrupt? Changes in water source of Lake Turkana (Kenya) during the African Humid Period inferred from Sr isotope ratios. *Quaternary Science Reviews* **174**, 1–12. <https://doi.org/10.1016/j.quascirev.2017.08.010>.
- Viste, E., Sorteberg, A., 2013. Moisture transport into the Ethiopian highlands. *International Journal of Climatology* **33**, 249–263. <https://doi.org/10.1002/joc.3409>.
- Vuille, M., Werner, M., Bradley, R.S., Keimig, F., 2005. Stable isotopes in precipitation in the Asian monsoon region. *Journal of Geophysical Research* **110**, D23108. <https://doi.org/10.1029/2005JD006022>.
- Wagner, B., Wennrich, V., Viehberg, F., Junginger, A., Kolvenbach, A., Rethemeyer, J., Schaebitz, F., Schmiedl, G., 2018. Holocene rainfall runoff in the central Ethiopian highlands and evolution of the River Nile drainage system as revealed from a sediment record from Lake Dendi. *Global and Planetary Change* **163**, 29–43. <https://doi.org/10.1016/j.gloplacha.2018.02.003>.
- Waterhouse, J.S., Cheng, S., Juchelka, D., Loader, N.J., Mccarroll, D., Switsur, V.R., Gautam, L., 2013. Position-specific measurement of oxygen isotope ratios in cellulose: isotopic exchange during heterotrophic cellulose synthesis. *Geochimica et Cosmochimica Acta* **112**, 178–191. <https://doi.org/10.1016/j.gca.2013.02.021>.
- Werdecker, J., 1962. Eine Durchquerung des Goba-Massivs in Südäthiopien. *Hermann von Wissmann-Festschrift, Tübingen* **1962**, 132–144.
- Williams, F.M., 2016. The Southeastern Highlands and the Ogaden. In: Williams, F.M. (Ed.), *Understanding Ethiopia: Geology and Scenery. Geoguide*. Springer International Publishing, Cham, pp. 153–170. [https://doi.org/10.1007/978-3-319-02180-5\\_15](https://doi.org/10.1007/978-3-319-02180-5_15).
- Wilson, K.E., Maslin, M.A., Leng, M.J., Kingston, J.D., Deino, A.L., Edgar, R.K., Mackay, A.W., 2014. East African lake evidence for Pliocene millennial-scale climate variability. *Geology* **42**, 955–958. <https://doi.org/10.1130/G35915.1>.
- Woldu, Z., Feoli, E., Nigatu, L., 1989. Partitioning an elevation gradient of vegetation from southeastern Ethiopia by probabilistic methods. *Plant Ecology* **81**, 189–198.
- Zech, M., Glaser, B., 2009. Compound-specific  $\delta^{18}\text{O}$  analyses of neutral sugars in soils using gas chromatography-pyrolysis-isotope ratio mass spectrometry: problems, possible solutions and a first application. *Rapid Communications in Mass Spectrometry* **23**, 3522–3532. <https://doi.org/10.1002/rcm.4278>.
- Zech, M., Mayr, C., Tuthorn, M., Leiber, K., Glaser, B., Leiber-Sauheitl, K., Glaser, B., et al., 2014a. Oxygen isotope ratios ( $^{18}\text{O}/^{16}\text{O}$ ) of hemicellulose-derived sugar biomarkers in plants, soils and sediments as paleoclimate proxy I: insight from a climate chamber experiment. *Geochimica et Cosmochimica Acta* **126**, 614–623. <https://doi.org/10.1016/j.gca.2013.10.048>.
- Zech, M., Tuthorn, M., Zech, R., Schlütz, F., Zech, W., Glaser, B., 2014b. A 16-ka  $\delta^{18}\text{O}$  record of lacustrine sugar biomarkers from the High Himalaya reflects Indian Summer Monsoon variability. *Journal of Paleolimnology* **51**, 241–251. <https://doi.org/10.1007/s10933-013-9744-4>.